Ecological Monographs, 87(4), 2017, pp. 632–664
© 2017 by the Ecological Society of America

An individual-based forest model to jointly simulate carbon and tree diversity in Amazonia: description and applications

Isabelle Maréchaux [1,2,3] and Jérôme Chave [1]

[1]*CNRS, Université Toulouse 3 Paul Sabatier, ENFA, UMR5174 EDB (Laboratoire Évolution & Diversité Biologique), 118 route de Narbonne, F-31062 Toulouse, France*
[2]*AgroParisTech-ENGREF, 19 avenue du Maine, F–75015 Paris, France*

Abstract. Forest dynamic models predict the current and future states of ecosystems and are a nexus between physiological processes and empirical data, forest plot inventories and remote-sensing information. The problem of biodiversity representation in these models has long been an impediment to a detailed understanding of ecosystem processes. This challenge is amplified in species-rich and high-carbon tropical forests. Here we describe an individual-based and spatially explicit forest growth simulator, TROLL, that integrates recent advances in plant physiology. Processes (carbon assimilation, allocation, reproduction, and mortality) are linked to species-specific functional traits, and the model was parameterized for an Amazonian tropical rainforest. We simulated a forest regeneration experiment from bare soil, and we validated it against observations at our sites. Simulated forest regeneration compared well with observations for stem densities, gross primary productivity, aboveground biomass, and floristic composition. After 500 years of regrowth, the simulated forest displayed structural characteristics similar to observations (e.g., leaf area index and trunk diameter distribution). We then assessed the model's sensitivity to a number of key model parameters: light extinction coefficient and carbon quantum yield, and to a lesser extent mortality rate, and carbon allocation, all influenced ecosystem features. To illustrate the potential of the approach, we tested whether variation in species richness and composition influenced ecosystem properties. Overall, species richness had a positive effect on ecosystem processes, but this effect was controlled by the identity of species rather by richness per se. Also, functional trait community means had a stronger effect than functional diversity on ecosystem processes. TROLL should be applicable to many tropical forests sites, and data requirement is tailored to ongoing trait collection efforts. Such a model should foster the dialogue between ecology and the vegetation modeling community, help improve the predictive power of models, and eventually better inform policy choices.

Key words: *Amazonia; biodiversity; biomass; functional traits; individual-based model; negative density dependence; plant community dynamics; productivity; regeneration; sensitivity analysis; spatially explicit; tropical forest.*

Introduction

Much of the uncertainty in the current and future status of the carbon cycle is associated to the dynamics of terrestrial vegetation and its response to climate (Fisher et al. 2014). Tropical forests play a fundamental role in regional and global biogeochemical cycles (Malhi et al. 2008, Saatchi et al. 2011, Harper et al. 2013), they host over half of the Earth's biodiversity (Scheffers et al. 2012), and they are increasingly altered by deforestation and degradation (Laurance et al. 2014, Lewis et al. 2015). For these reasons, tropical forests exemplify several of the major challenges in global environmental governance.

Terrestrial biosphere models play a foremost role in understanding how current forcings will alter vegetation dynamics and biogeochemical cycles (Friedlingstein et al. 2013), and in conveying evidence-based knowledge to policy makers. However, the development of these models is still facing major challenges in tropical forests and elsewhere, in part related to our still-limited understanding of plant physiological and ecological processes (Rogers et al. 2017), but also to the way dynamic vegetation models (DVMs) have been implemented (Prentice et al. 2007). DVMs describe vegetation dynamics at a coarse spatial grain (of typically 1° × 1° resolution) and they still often use a big-leaf approach to describe the balance in carbon, water, and energy.

Also DVMs aggregate terrestrial plant diversity into less than a dozen plant functional types (PFTs), broadly defined by their geographical affinity, deciduousness, and physiology (Sitch et al. 2003, Clark et al. 2011). However, leaf and stem functional traits that govern plant physiology display a wide spectrum of variation within PFTs, and particularly so in tropical ecosystems (Fyllas et al. 2009, Baraloto et al. 2010, Díaz et al. 2016). By ignoring

Manuscript received 20 December 2016; revised 20 June 2017; accepted 23 June 2017. Corresponding Editor: Jonathan M. Levine.
[3] E-mail: isabelle.mj.marechaux@gmail.com

species diversity, vegetation models may fail to describe features of vegetation structure or dynamics, such as productivity (Morin et al. 2011, Grace et al. 2016), biomass (Poorter et al. 2015), or stability (Loreau and de Mazancourt 2013, Morin et al. 2014). Including functional diversity in DVMs should help increase their predictive power (Moorcroft 2006, Purves and Pacala 2008). New-generation models could even jointly model elemental cycles and the dynamics of biodiversity (Harfoot et al. 2014, Van Bodegom et al. 2014, Mokany et al. 2016). Here, we aim to bring a novel contribution to this research challenge, by implementing a scalable and physiology-based individual-based forest simulator (Shugart 1984, Bugmann 2001) that jointly simulates physiological processes and tree diversity.

Because they integrate finer-grained details of forest spatial heterogeneity and diversity than DVMs, individual-based forest models are useful for assimilating ecological data (Pacala et al. 1996), and remote-sensing data (Shugart et al. 2015). They can also be used to upscale ecosystem processes at regional scale (Moorcroft et al. 2001, Sato et al. 2007, Strigul et al. 2008). However, individual-based forest simulators have seldom been designed to explore vegetation responses to multiple interacting climate drivers, since tree growth is often modeled using empirical equations, rather than explicit processes of carbon assimilation and allocation (Le Roux et al. 2001, Pretzsch et al. 2015). Also, it has been argued that individual-based forest models require too much computer power to be used at large scales (Strigul et al. 2008). With advances in plant physiology and in computer power, both limitations can now be critically reappraised (Shugart et al. 2015).

A number of steps have been taken to bridge the gap between DVMs and finer-grained models so as to account for demographic stochasticity (Strigul et al. 2008), but also to more efficiently assimilate information from large plant trait databases (Kattge et al. 2011). In some new-generation vegetation models, PFTs have been replaced by a trait continuum approach to model cohorts of individuals (Scheiter et al. 2013, Verheijen et al. 2013, Fyllas et al. 2014), or individual trait combinations have been constrained by documented plant economics spectra (Pavlick et al. 2013, Sakschewski et al. 2015). These modeling approaches represent promising steps toward the building of new-generation DVMs (van Bodegom et al. 2012, 2014). However, these models take a "taxonomy-free" approach in the description of biological diversity, ignoring species-level differences and focusing on the continuum of traits. While this is an interesting simplification, it is unclear how ecological processes, such as competition, facilitation, or multitrophic interactions, can be included in this approach.

To illustrate this point, it has been abundantly documented that natural plant enemies, such as herbivores or pathogens, tend to negatively impact abundant species more than rare species, hence promoting the high biodiversity of tropical forests (Janzen 1970, Connell 1971, Harms et al. 2000, Wright 2002, Bagchi et al. 2014, Comita et al. 2014). This negative density dependence is thought to have direct implications for biodiversity maintenance and also potentially for the carbon cycle, as has been demonstrated for North American forests (Hicke et al. 2012), and for other ecosystem services (Boyd et al. 2013). Few individual-based forest models have considered this ecological process (but see Lischke and Löffler 2006). Another connection between biodiversity and ecosystem functioning is the hypothesis that species-rich forests have higher biomass, higher productivity, and more resilience to disturbances than those with a few species as shown experimentally (Hooper et al. 2005, Scherer-Lorenzen et al. 2007), and in natural vegetation (Vilà et al. 2007, Tobner et al. 2013, Toïgo et al. 2015), although rarely in tropical forests (but see Sapijanskas et al. 2014, Poorter et al. 2015, Chiang et al. 2016). A mechanistic understanding of these ecological processes and their ecosystem-wide implications is difficult, and trait-based DVMs are not ideally suited to capture such ecological processes. Individual-based vegetation models are a logical option to test these hypotheses (Morin et al. 2011, Forrester 2014).

In this contribution, we integrate physiological processes underlying plant responses to the environment into the forest growth simulator TROLL (Chave 1999), an individual-based and spatially explicit forest model operating at an even finer-grained representation of space and forest structure than gap models usually do. Ecological complexity is much simpler to address at the spatial scale of TROLL than in coarse-grained vegetation models. Also, TROLL is uniquely suited to data–model comparisons, since its inputs and outputs closely match the scale and resolution of field measurements, from organism scale to community scale (Clark et al. 2017). We provide a field parameterization that depends of species identity for a tropical rainforest. This version of the TROLL model simultaneously simulates ecosystem processes and vegetation diversity, paving the way to new practical and theoretical applications. We here (1) describe the model structure and its parameterization; (2) we simulate the regeneration of a tropical rainforest from bare soil, and validate it against a range of observations at our sites; (3) we assess model sensitivity to a number of key global parameters, and to the inclusion of negative density-dependence processes; (4) finally, we conduct a virtual biodiversity experiment by testing the influence of species composition on ecosystem properties. These results shed light on the potential contribution of a model such as TROLL to the challenge of improving predictive next-generation terrestrial biosphere models.

Model Description

Overview

TROLL belongs to the family of individual-based and spatially explicit forest growth simulators, along with

SORTIE (Pacala et al. 1996, Uriarte et al. 2009) and FORMIND (Köhler and Huth 1998, Fischer et al. 2016). The model was named after German plant morphologist Wilhelm Troll (1897–1978) and his brother, tropical ecologist Carl Troll (1899–1975). TROLL simulates the life cycle of individual trees (recruitment, growth, seed production, and death) >1 cm diameter. Trees grow in a forest light environment that is computed explicitly within a voxel space of 1 m^3. Each tree is defined by its age, and a set of biometric state variables (dbh, height, crown radius and crown depth, leaf area; Fig. 1). As in most forest simulators, tree geometry is set by allometric equations, but leaf area varies dynamically within each crown, as a balance between allocation and losses (leaf fall). At most, one tree can establish in each 1 × 1 m pixel. In contrast with previous forest simulators, tree growth is simulated from an explicit carbon balance calculation (photosynthetic assimilation plus allocation), with assimilation computed over half-hourly periods of a representative day. This, in turn influences the environment at the next timestep, which is here set to one month. Seedlings below the 1-cm size class are not modeled explicitly, but are part of a seed/seedling pool. In this version of TROLL, belowground processes are not explicitly represented, and herbaceous plants, epiphytes, and lianas are not included.

A species label is attached to each tree and is inherited from the mother tree through the seed. With this species label are associated seven species-specific parameters, namely leaf mass per area, leaf nitrogen and phosphorus content, wood specific gravity, threshold dbh beyond which growth efficiency declines, asymptotic height, and a parameter of the dbh–height allometry (Table 1). These traits can be directly obtained from field measurements (see *Perspectives in forest biodiversity modeling*).

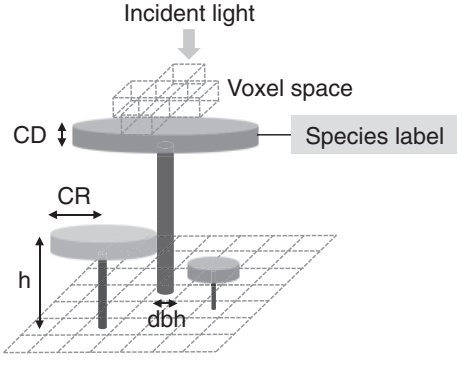

FIG. 1. Representation of individual trees in a spatially explicit grid in TROLL. Each tree is composed of a trunk and a crown, with cylinder shapes. The crown and trunk dimensions (crown radius, CR; crown depth, CD; height, h; diameter at breast height, dbh) are updated at each timestep, depending on the assimilated carbon that is allocated to growth, and following allometric relationships. Each tree has a species label with species-specific parameters (see Table 1). Light diffusion is computed explicitly at each timestep and within each voxel from the canopy top to the ground.

TABLE 1. Species-specific parameters provided in input of the TROLL model.

Abbreviation	Description	Units
LMA	leaf mass per area	g/m^2
N	leaf nitrogen content per dry mass	mg/g
P	leaf phosphorous content per dry mass	mg/g
wsg	wood specific gravity	g/cm^3
dbh_{thresh}	diameter at breast height threshold	m
h_{lim}	asymptotic height	m
a_h	parameter of the tree-height-dbh allometry	m

Note: All data are from the BRIDGE (Baraloto et al. 2010) and TRY (Kattge et al. 2011) data sets, except some species values of LMA, N, and P (I. Maréchaux and J. Chave, *unpublished data*).

The source code is written in C++ and is *available online* (version 2.3.2).[4] Visualization, statistical analysis, and data processing were performed in R version 3.0.2 (R Core Team 2013). In the following subsections, we detail the model representation of processes and discuss the assumptions. Model parameterization, validation data and simulation set-ups are presented in the next section.

Modeling the abiotic environment

Within-canopy heterogeneity is explicitly modeled. The physical space in which trees grow is described as a three-dimensional grid discretized into voxels 1 × 1 × 1 m (i.e., 1 m^3, Fig. 1). The maximal tree size (up to 60–80 m), serves as an upper threshold for the upward extension of the voxel space.

For each tree crown, leaf area density is deduced from tree geometry assuming that a tree distributes its leaf area uniformly across the voxels occupied by its crown (voxel-mean leaf density LD, in m^2/m^3). Cumulating over all the trees, leaf area density (leaf area per voxel; in m^2/m^3) is computed within each voxel v, and is denoted LAD(v). The vertical sum of LAD, upward from each voxel, defines

$$\mathrm{LAI}(v) = \sum_{v'=v}^{\infty} \mathrm{LAD}(v'). \quad (1)$$

LAI(v) for ground-layer voxels v, commonly called LAI (leaf area index), is the cumulative leaf area density down to the ground level (leaf area per ground area, in m^2/m^2), and is a common metric in forestry. LAI typically ranges between 5 and 7 in closed tropical canopy-forests (Clark et al. 2008), and nowadays, terrestrial lidar scanning technology allows a direct measurement of LAD(v) in forests (Calders et al. 2015).

To compute carbon assimilation, we compute the daily course of variation in light intensity (photosynthetic photon flux density, PPFD, in μmol photons·m^{-2}·s^{-1}), temperature (T, in degrees Celsius), and vapor pressure deficit (VPD, in kPa) within each voxel of the canopy and

[4] https://github.com/TROLL-code/TROLL

for one representative day per month (Appendix S1). To this end, we model the within-canopy variation in PPFD as a local Beer-Lambert extinction law

$$\mathrm{PPFD}_{\mathrm{max,month}}(v) = \mathrm{PPFD}_{\mathrm{top,max,month}} \times \exp[-k \times \mathrm{LAI}(v)] \quad (2)$$

where the monthly average of the daily maximum incident PPFD at top canopy ($\mathrm{PPFD}_{\mathrm{top,max,month}}$) is prescribed from measurements. We assume a uniform and constant extinction rate k (values for each parameter are reported in Table 2), even though it is expected to vary with zenith angle and species leaf inclination angle (Meir et al. 2000, Kitajima et al. 2005). Given the importance of light limitation in the understory of tropical forests, we expect the model to be sensitive to the choice of k. In this version of the model, we considered only vertical light diffusion, ignoring more complex light models within vegetation canopies (Canham et al. 1994, Brunner 1998) or full radiative transfer models (Gastellu-Etchegorry et al. 1996, Lewis 1999, Mercado et al. 2009*a*, Widlowski et al. 2013). PPFD, temperature, and VPD decrease with forest canopy depth (v) and we describe their intra-day variation at half-hourly time steps t for a representative day every month, thus the microenvironment is described by $\mathrm{PPFD}_{\mathrm{month}}(v,t)$, $T_{\mathrm{month}}(v,t)$ and $\mathrm{VPD}_{\mathrm{month}}(v,t)$ (Appendix S1).

In the future, coupling TROLL with an energy transfer model could simplify this representation of the microenvironment. Alternatively, the model could input empirically measured half-hourly data sets of PPFD, T, and VPD. In its current version, TROLL does not explicitly calculate the water balance in the soil and the soil–plant–atmosphere water column (Williams et al. 1996, Granier et al. 1999, Laio et al. 2001). It also ignores the dynamics of nutrients in the soil (Goll et al. 2012), and assumes fixed species-specific leaf nutrient concentrations. These additions are postponed to subsequent contributions.

Photosynthetic carbon uptake by plants: leaf-level theory

The first version of TROLL assumed an empirical form of the growth of tree trunk diameters, as in most forest gap models (Chave 1999). Here, we include a description of the carbon uptake for each plant, with the Farquhar, von Caemmerer, and Berry model of C_3 photosynthesis (Farquhar et al. 1980). Gross carbon assimilation rate (A, μmol $CO_2 \cdot m^{-2} \cdot s^{-1}$) is limited by either Rubisco activity (A_v), or RuBP regeneration (A_j)

$$\begin{aligned} A &= \min\{A_v, A_j\} \\ A_v &= V_{\mathrm{cmax}} \times \frac{c_i - \Gamma^*}{c_i + K_m} \\ A_j &= \frac{J}{4}\frac{c_i - \Gamma^*}{c_i + 2\Gamma^*} \end{aligned} \quad (3)$$

where V_{cmax} is the maximum rate of carboxylation ($\mu\mathrm{molCO_2 \cdot m^{-2} \cdot s^{-1}}$), c_i the CO_2 partial pressure at carboxylation sites, Γ* the CO_2 compensation point in the absence of dark respiration, K_m the apparent kinetic constant of the Rubisco (von Caemmerer 2000), and J the electron transport rate (μmol electrons$\cdot m^{-2} \cdot s^{-1}$), which depends on PPFD through

$$J = \frac{1}{2\theta}\left[\alpha \times \mathrm{PPFD} + J_{\mathrm{max}} - \sqrt{\begin{array}{c}(\alpha \times \mathrm{PPFD} + J_{\mathrm{max}})^2 \\ -4\theta \times \alpha \times \mathrm{PPFD} \times J_{\mathrm{max}}\end{array}}\right]. \quad (4)$$

J_{max} is the maximal electron transport capacity (μmol electrons$\cdot m^{-2} \cdot s^{-1}$), θ the curvature factor, and α the apparent quantum yield to electron transport (mol electrons/mol photons). In the following, we use ϕ, the apparent quantum yield for C fixation (mol C/mol photons), which is the initial slope of the photosynthetic assimilation plotted against incident irradiance. Note that four electrons are needed to regenerate RuBP, so $\alpha = 4\phi$. In this photosynthesis model, ϕ, V_{cmax}, and J_{max} are empirical parameters that represent a large source of uncertainty in vegetation models (Zaehle et al. 2005, Mercado et al. 2009*b*, Rogers et al. 2017).

Carbon assimilation by photosynthesis is limited by the CO_2 partial pressure at carboxylation sites, which is controlled by stomatal transport as modeled by the diffusion equation

TABLE 2. Global parameters used in TROLL. When specified, values in brackets correspond to the distribution range used for the sensitivity analysis.

Abbreviation	Description	Units	Values	Source
k	light extinction coefficient, used in light diffusion Beer-Lambert law		0.90 [0.50;0.95]	Wirth et al. (2001), Cournac et al. (2002)
ϕ	apparent quantum yield for C fixation	mol C/mol photons	0.075 [0.04;0.09]	Domingues et al. (2014)
g_1	stomatal conductance parameter	$kPa^{1/2}$	3.77 [2;5]	Lin et al. (2015)
f_{wood}	fraction of NPP allocated to wood growth		0.35 [0.20;0.45]	Aragão et al. (2009), Malhi et al. (2011)
f_{canopy}	fraction of NPP allocated to canopy, including leaves†, fruits and twigs		0.30 [0.20;0.45]	Aragão et al. (2009), Malhi et al. (2011)
m	maximal basal mortality rate		0.025 [0.005;0.045]	

†The fraction of NPP allocated to leaves only is set at $0.68 \times f_{\mathrm{canopy}}$ according to Chave et al. (2008*b*, 2010).

$$A = g_s(c_a - c_i) \quad (5)$$

with g_s the stomatal conductance to CO_2 (mol $CO_2 \cdot m^{-2} \cdot s^{-1}$). In most DVMs, leaf stomatal conductance is modeled empirically as a function of the VPD (Ball et al. 1987, Leuning 1995). Instead we use the model developed by Medlyn et al. (2011)

$$g_s = g_0 + \left(1 + \frac{g_1}{\sqrt{\text{VPD}}}\right)\frac{A}{c_a} \quad (6)$$

where g_0 and g_1 are parameters. Medlyn et al. (2011)'s model results from an optimization argument, according to which stomata should act to maximize carbon gain while minimizing water loss (Cowan and Farquhar 1977). Assuming $g_0 \approx 0$, an empirically reasonable assumption, and coupling Eqs. 5 and 6, this leads to

$$\frac{c_i}{c_a} = \frac{g_1}{g_1 + \sqrt{\text{VPD}}} \quad (7)$$

so the c_i/c_a ratio declines as VPD increases. Focusing on the light-limited part of the Farquhar model, this shows that $g_1 \propto \sqrt{\Gamma^*}$, which suggests that g_1 increases with temperature. Using a different optimal theory pathway and focusing on the Rubisco-limited part of the Farquhar model, Prentice et al. (2014) derived the same expression as Eq. 7, but with $g_1 \propto \sqrt{K_m}$, also suggesting a strong positive dependence of g_1 on temperature.

Photosynthetic carbon uptake by plants: leaf-level parameterization

Photosynthetic capacity depends on leaf nutrient content and other leaf traits (Reich et al. 1997, Wright et al. 2004). In tropical forest environments, Domingues et al. (2010) suggested that V_{cmax} and J_{max} are colimited by the leaf concentration of nitrogen (N) and phosphorus (P)

$$\log_{10} V_{cmax-M} = \min\left\{\begin{array}{l} -1.56 + 0.43 \times \log_{10}\text{N} - 0.37 \times \log_{10}\text{LMA}; \\ -0.80 + 0.45 \times \log_{10}\text{P} - 0.25 \times \log_{10}\text{LMA} \end{array}\right\} \quad (8)$$

$$\log_{10} J_{max-M} = \min\left\{\begin{array}{l} -1.50 + 0.41 \times \log_{10}\text{N} - 0.45 \times \log_{10}\text{LMA}; \\ -0.74 + 0.44 \times \log_{10}\text{P} - 0.32 \times \log_{10}\text{LMA} \end{array}\right\} \quad (9)$$

with V_{cmax-M} and J_{max-M} the photosynthetic capacities at 25°C of mature leaves on a leaf dry mass basis, in μmol $CO_2 \cdot g^{-1} \cdot s^{-1}$ and μmol electrons $\cdot g^{-1} \cdot s^{-1}$, respectively. N and P are the leaf nitrogen and phosphorous contents in mg/g, and LMA is the leaf mass per area in g/cm^2. V_{cmax-M} and J_{max-M} can be converted into area-based V_{cmax} and J_{max} by multiplying by LMA. Because N, P, and LMA vary across species, these photosynthetic capacity parameters are also species specific (Table 1). Recent modeling studies have implemented this model for Amazonian forests (Mercado et al. 2011, Fyllas et al. 2014). To account for variation of V_{cmax} and J_{max} with temperature, we used the formulas of Bernacchi et al. (2003) and enzymatic kinetic constant values and their temperature relationships of von Caemmerer (2000, Domingues et al. 2010; see Appendix S2). Long-term acclimation to temperature is not included here as simulations were conducted in a stable climate, and is left for future developments (Kattge and Knorr 2007, Smith and Dukes 2013).

The stomatal conductance model (Eqs. 5–6) depend on g_1, which is expected to vary with whole-plant water-use efficiency, or marginal carbon cost of water use. The parameter g_1 has been found to vary among plant functional types (Lin et al. 2015). Given the lack of direct measurements of g_1 at the species level and of a robust relationship with other functional traits, we here used a fixed mean value of g_1 (Table 2). We expect a high sensitivity of the stomatal conductance model to the value of g_1 (Kala et al. 2015, 2016, Knauer et al. 2015).

Combining Eqs. 3–9 for each tree crown voxel, leaf carbon assimilation A_l is finally computed for each tree and within each crown layer l (in μmol $CO_2 \cdot m^{-2} \cdot s^{-1}$), as follows in Eq. 10:

where the microclimatic variables are taken from Appendix S1 and A_l averaged across the n_v voxels within crown layer l, and over the half-hourly intervals of a typical day (where t_M represents the number of half-hourly values of daytime).

Autotrophic respiration

Plants metabolize a large fraction of their carbon uptake for maintenance and growth, and this autotrophic respiration typically represents 30–65% of the gross primary productivity (Malhi 2012). It varies strongly among species, within and across sites (Slot et al. 2013, Atkin et al. 2015), and with the environment (Atkin et al. 2005, Wright et al. 2006). However, this process constitutes a major source of uncertainty in

$$A_l = \frac{1}{n_v \times t_M} \times \sum_v \sum_{t=1}^{t_M} A\left(\text{PPFD}_{\text{month}}(v,t), \text{VPD}_{\text{month}}(v,t), T_{\text{month}}(v,t)\right) \quad (10)$$

modeling carbon fluxes (Huntingford et al. 2013, Atkin et al. 2014). As in most vegetation models, we partitioned autotrophic respiration into maintenance respiration and growth respiration, acknowledging that they come from the same biochemical pathways (Amthor 1984, Thornley and Cannell 2000).

Maintenance respiration ($R_{\text{maintenance}}$) is usually inferred empirically (Meir et al. 2001, Cavaleri et al. 2008, Slot et al. 2013, Weerasinghe et al. 2014) and has seldom been documented for stem and roots. Atkin et al. (2015) compiled a database of mature leaf dark respiration and associated leaf traits for 899 species of 100 sites worldwide, spanning a wide range of biomes, including tropical forests. We used their "broadleaved trees" empirical model to compute leaf maintenance respiration for each species

$$R_{\text{leaf-M}} = 8.5341 - 0.1306 \times \text{N} - 0.5670 \times \text{P} - 0.0137 \times \text{LMA} + 11.1 \times V_{\text{cmax-M}} + 0.1876 \times \text{N} \times \text{P} \quad (11)$$

with $R_{\text{leaf-M}}$ the species-specific leaf dark respiration rate on a dry mass basis and at reference temperature of 25°C, in nmol $CO_2 \cdot g^{-1} \cdot s^{-1}$. The other terms are as in Eqs. 8–9. Multiplying $R_{\text{leaf-M}}$ by LMA gives a species-specific area-based R_{leaf} (in μmol $C \cdot m^{-2} \cdot s^{-1}$). For consistency, we used the same temperature dependencies for leaf respiration as in Atkin et al. (2015; see also Heskel et al. 2016). We assumed leaf respiration rate during day light to be 40% of leaf respiration in the dark at the typical range of temperatures at our site (Atkin et al. 2000). Total leaf respiration per timestep is then calculated by explicitly accounting for the length of daylight.

Stem maintenance respiration (R_{stem}, in μmol C/s) is modeled assuming a constant respiration rate per volume of sapwood (Ryan et al. 1994), so that

$$R_{\text{stem}} = 39.6 \times \pi \times \text{ST} \times (\text{dbh} - \text{ST}) \times (\text{h} - \text{CD}) \quad (12)$$

with dbh, h, CD, ST the tree diameter at breast height, total tree height, crown depth, and sapwood thickness, respectively (all in m). We assumed that ST = 0.04 m for trees with a dbh > 30 cm and that ST increases with dbh from 0 to 0.04 m for smaller trees in agreement with empirical studies (Granier et al. 1996, Meir and Grace 2002). Stem respiration response to temperature was modeled using a Q_{10} value of 2.0 (Ryan et al. 1994, Meir and Grace 2002). Stahl et al. (2011) reported that R_{stem} varies among individual trees, even when controlling for sapwood volume. However, in the absence of a more precise understanding of the causes of variation, we used Eq. 12. Also, Stahl et al. (2010) and van der Sande et al. (2015) showed that ST can vary significantly across conspecific trees and among species, but the model assumed here is considered a reasonable first step.

Fine root maintenance respiration was assumed to be half of leaf maintenance respiration (Malhi 2012), and coarse root and branch maintenance respirations were assumed to account for one-half of stem respiration (Meir and Grace 2002, Cavaleri et al. 2006, Asao et al. 2015). Finally, growth respiration (R_{growth}) was assumed to account for 25% of the carbon uptake by photosynthesis (gross primary productivity) minus the maintenance respiration (Cannell and Thornley 2000). These assumptions are commonly made in the literature, but in the future, it would be desirable to provide more precise models.

Net carbon uptake: whole-tree integration and allocation

At each timestep, individual net primary production of carbon NPP_{ind} (in g C) is obtained by the following balance equation:

$$\text{NPP}_{\text{ind}} = \text{GPP}_{\text{ind}} - R_{\text{maintenance}} - R_{\text{growth}}. \quad (13)$$

To calculate NPP_{ind}, area-based GPP and leaf respiration must be summed over the crown's total leaf area. Each tree's total leaf area (LA) is partitioned into three pools corresponding to the following leaf age classes: young, mature, and old leaves, so that $\text{LA} = \text{LA}_{\text{young}} + \text{LA}_{\text{mature}} + \text{LA}_{\text{old}}$ (all in m^2). Young leaves and old leaves have lower photosynthetic capacities and activities than mature leaves (Kitajima et al. 1997, 2002, Doughty and Goulden 2008, De Weirdt et al. 2012, Wu et al. 2016). We assumed that young and mature leaves have assimilation and respiration rates one-half that of mature leaves (see Eqs. 3 and 11), so that Eq. 14 below

where h is tree height, CD tree crown depth, and $\lfloor x \rfloor$ is the rounding function, Δt the duration of a timestep (in yr). The factor 189.3 converts a rate from μmol $CO_2 \cdot m^{-2} \cdot s^{-1}$ to g $C \cdot m^{-2} \cdot yr^{-1}$ (with 12 the molar mass of C, an average number of days per year of 365.25, and assuming 12 h of assimilation per day throughout the year). At each timestep, respiration terms are also converted into g C.

Carbon allocation to plant organs is prescribed by fixed factors derived from empirical studies at our sites (Chave et al. 2008*b*) or elsewhere in Amazonia (Aragão et al. 2009, Malhi et al. 2011, 2015, Table 2). Carbon allocated to wood is converted into an increment of stem volume, ΔV in m^3, as follows:

$$\text{GPP}_{\text{ind}} = 189.3\ \Delta t \times \sum_{l=\lfloor h-\text{CD} \rfloor+1}^{\lfloor h \rfloor} [A_l] \times \left(0.5 \times \text{LA}_{\text{young}} + \text{LA}_{\text{mature}} + 0.5 \times \text{LA}_{\text{old}}\right) \quad (14)$$

$$\Delta V = 10^{-6} \times \frac{f_{\text{wood}} \times \text{NPP}_{\text{ind}}}{0.5 \times \text{wsg}} \times \text{Senesc(dbh)} \quad (15)$$

where f_{wood} is the fixed fraction of NPP allocated to aboveground woody growth (i.e., stem and branches), wsg is the species-specific wood specific gravity (g/cm^3; Table 1), and the factor 0.5 converts dry biomass units into carbon units (Elias and Potvin 2003, Thomas and Martin 2012). We assumed that the largest trees cannot allocate carbon as efficiently into growth, reflecting empirical evidence of a size-related relative growth decline in trees (Yoda et al. 1965, Ryan et al. 1997, Mencuccini et al. 2005, Woodruff and Meinzer 2011, Stephenson et al. 2014): trees cannot exceed the dbh given by $\text{dbh}_{\text{max}} = \frac{3}{2}\text{dbh}_{\text{thresh}}$ and they are assumed to be in the declining phase if $\text{dbh}_{\text{thresh}} \leq \text{dbh} \leq \frac{3}{2}\text{dbh}_{\text{thresh}}$. Here $\text{dbh}_{\text{thresh}}$ is a species-specific threshold (Table 1). If $\text{dbh} \leq \text{dbh}_{\text{thresh}}$, then $\text{Senesc(dbh)} = 1$. Else, if $\text{dbh} > \text{dbh}_{\text{thresh}}$, then $\text{Senesc(dbh)} = \max\left(0; 3 - 2\frac{\text{dbh}}{\text{dbh}_{\text{thresh}}}\right)$.

Next, the fraction of NPP allocated to the tree canopy is denoted by f_{canopy} (Table 2), further decomposed into leaf, twig, and fruit production, i.e., $f_{\text{canopy}} = f_{\text{leaves}} + f_{\text{fruit}} + f_{\text{twigs}}$. Carbon allocated to leaf production results in a new young leaf pool, and leaf area dynamics obey the following equations:

$$\begin{aligned}
\Delta\text{LA}_{\text{young}} &= \frac{2 \times f_{\text{leaves}} \times \text{NPP}_{\text{ind}}}{\text{LMA}} - \frac{\text{LA}_{\text{young}}}{\tau_{\text{young}}} \\
\Delta\text{LA}_{\text{mature}} &= \frac{\text{LA}_{\text{young}}}{\tau_{\text{young}}} - \frac{\text{LA}_{\text{mature}}}{\tau_{\text{mature}}} \\
\Delta\text{LA}_{\text{old}} &= \frac{\text{LA}_{\text{mature}}}{\tau_{\text{mature}}} - \frac{\text{LA}_{\text{old}}}{\tau_{\text{old}}}
\end{aligned} \quad (16)$$

where τ_{young}, τ_{mature}, and τ_{old} are species-specific residence times in each class (in yr) and LL is the species-specific leaf lifespan (in yr), so that $\text{LL} = \tau_{\text{young}} + \tau_{\text{mature}} + \tau_{\text{old}}$. In this model, we infer LL from LMA for each species, using the equation proposed by Reich et al. (1997), τ_{young} was fixed to 1/12 yr for all species (one month; Doughty and Goulden 2008, Wu et al. 2016), and τ_{mature} as one-third of the leaf lifespan. The loss term $\text{LA}_{\text{old}}/\tau_{\text{old}}$ corresponds to the rate of leaf litterfall at each timestep. Thus, litterfall results from the dynamics of leaf biomass and specific leaf lifespans. This is unlike Wu et al. (2016) where litterfall was prescribed, Forrester and Tang (2016) where litterfall was a constant fraction of leaf stock, or De Weirdt et al. (2012) where it was assumed equal to the biomass allocated to leaves (implying a constant total leaf area). Belowground carbon allocation was not included explicitly in this version of the model. As the allocation factors f_{wood} and f_{canopy} drive the pathway from tree productivity to aboveground biomass (AGB) and structure, we expect a high sensitivity of the model to these parameters.

Tree growth and allometries

Trunk diameter growth in dbh, Δdbh, is computed from ΔV (Eq. 15), as follows. We assumed that tree height is inferred from the dbh value using a Michaelis-Menten equation

$$h = h_{\text{lim}} \frac{\text{dbh}}{\text{dbh} + a_h} \quad (17)$$

with h_{lim} and a_h, species-specific parameters derived from local measurements on standing trees (Baraloto et al. 2010, Table 1). Note that since $\text{dbh} \leq \frac{3}{2}\text{dbh}_{\text{thresh}}$, h is bounded upward by a value that we call $h_{\text{max}} = h_{\text{lim}} \frac{3\text{dbh}_{\text{thresh}}}{3\text{dbh}_{\text{thresh}} + 2a_h}$. Since $V = C\pi\left(\frac{\text{dbh}}{2}\right)^2 h$, then

$$\begin{aligned}
\Delta V &= C\frac{1}{2}\pi h \times \text{dbh} \times \Delta\text{dbh} + C\pi\left(\frac{\text{dbh}}{2}\right)^2 \Delta h \\
&= V\frac{\Delta\text{dbh}}{\text{dbh}}\left(3 - \frac{\text{dbh}}{\text{dbh} + a_h}\right)
\end{aligned} \quad (18)$$

or, equivalently, $\frac{\Delta V}{V} = \frac{\Delta\text{dbh}}{\text{dbh}}\left(3 - \frac{h}{h_{\text{lim}}}\right)$. Here, C is a form factor (Chave et al. 2014: Eq. 5 therein). Hence, Δdbh can be deduced from ΔV directly from Eq. 18 above.

Tree crown dimensions are then updated using allometric equations. We used a single allometric relationship between crown radius and dbh, and between crown depth and tree height, as follows:

$$\text{CR} = 0.80 + 10.47 \times \text{dbh} - 3.33 \times \text{dbh}^2 \quad (19)$$

$$\begin{aligned}
\text{CD} &= -0.48 + 0.26 \times h \ (h \geq 5\,\text{m}); \\
\text{CD} &= 0.13 + 0.17 \times h \ (h < 5\,\text{m}).
\end{aligned} \quad (20)$$

Eqs. 19 and 20 are based on 168 measurements carried out in French Guiana (Chave et al. 2005; with RMSE = 0.67 m, $R^2 = 0.74$, $P < 10^{-15}$ and RMSE = 2.63 m, $R^2 = 0.38$, $P < 10^{-15}$ for Eqs. 19 and 20, respectively). Since we lacked species-specific information, we used the same relationships linking crown radius to dbh and crown depth to tree height across all species. For Eqs. 17, 19, and 20, tree allometry has motivated a great deal of literature (Feldpausch et al. 2011, Lines et al. 2012, Chave et al. 2014, Jucker et al. 2017), and tree crown architecture depends on ecological strategies (Bohlman and O'Brien 2006, Poorter et al. 2006, Iida et al. 2012). A future version of the model will integrate species-specific allometries for crown dimensions and improved allometric relations for total tree height.

Finally, the mean leaf density within the crown (LD, in m^2/m^3) is computed as

$$\text{LD} = \frac{\text{LA}_{\text{young}} + \text{LA}_{\text{mature}} + \text{LA}_{\text{old}}}{\pi \times CR^2 \times \text{CD}}. \quad (21)$$

This variable depends on crown volume and total leaf area, assuming a uniform distribution of leaf area within the crown.

Mortality

Mortality processes are complex and still incompletely represented in current vegetation models, although they play a key role in forest structure and carbon balance (Delbart et al. 2010, Friend et al. 2014, Sevanto et al. 2014, Johnson et al. 2016). At each timestep, each tree simulated in TROLL has a probability to die, computed through the following death rate (in events/yr; Sheil et al. 1995):

$$d = d_{\mathrm{b}} + d_{\mathrm{NDD}} + d_{\mathrm{starv}} + d_{\mathrm{treefall}} \tag{22}$$

where d_{b} is a background death rate, d_{NDD} represents death due to negative density dependence, d_{starv} represents death due to carbohydrate shortage (carbon starvation), and d_{treefall} represents death due to treefall (including trees indirectly killed by neighboring fallen trees).

Background mortality d_{b} varies greatly among species, and we here assume that it is negatively correlated with species-specific wood density, as observed pan-tropically (King et al. 2006, Poorter et al. 2008, Kraft et al. 2010, Wright et al. 2010). This dependence illustrates a trade-off between investment into construction costs and risk of mortality (Chave et al. 2009). More precisely, we here assumed the following simple relationship:

$$d_{\mathrm{b}} = m \times \left(1 - \frac{\mathrm{wsg}}{\mathrm{wsg}_{\mathrm{lim}}}\right) \tag{23}$$

where m (in events/yr) is the reference background mortality rate for a species with very low wood density. It was tuned to fit observations of overall stem mortality rates. The parameter $\mathrm{wsg}_{\mathrm{lim}}$ is a value large enough so that d_{b} always remains positive (here set at 1).

In addition, we simulated mortality caused by all biotic negative-density-dependent factors (term d_{NDD}). The fitness of abundant species is reduced because they tend to attract more of their specific predators or pathogens (Wright 2002, Gonzalez et al. 2010, Zhu et al. 2015). Density dependence is strongest among conspecific individuals (Comita et al. 2010, Gonzalez et al. 2010, Paine et al. 2012). Here, we hypothesize that basal area is a good proxy for modeling negative density dependence and that this effect is identical across species (Comita and Hubbell 2009). At each site i and species s, we computed the term:

$$\mathrm{NDD}_{i,s} = \frac{1}{\pi R^2 \mathrm{BA}} \sum_{\substack{j \\ \text{trees of species } s \\ \text{with } d_{i,j} < R}} \mathrm{BA}_j \tag{24}$$

where BA_j is the basal area of a conspecific neighboring tree j, BA is the mean basal area of the stand (m^2/ha), and R is the radius of the neighborhood, set to 15 m (Uriarte et al. 2004, Comita and Hubbell 2009, Zhu et al. 2015). From Eq. 24, we computed d_{NDD} as follows:

$$d_{\mathrm{NDD}} = \Delta_d \times \mathrm{NDD}_{i,s}\left(1 - 2\frac{\mathrm{dbh}}{\mathrm{dbh}_{\mathrm{thresh}}}\right) \tag{25}$$

where Δ_d determines the strength of NDD on mortality. Here, we assume that d_{NDD} decreases linearly with the size of the focal tree (Uriarte et al. 2004, Zhu et al. 2015) and equals 0 when it reaches a size of $\mathrm{dbh}_{\mathrm{thresh}}/2$.

A tree can also die because of carbohydrate shortage in case of prolonged stress (term d_{starv} in Eq. 22). For each stem, we record the duration during which the tree is under a negative carbon balance, i.e., the number of consecutive timesteps with $\mathrm{NPP}_{\mathrm{ind}} < 0$ (Eq. 13). When the stress duration exceeds leaf lifespan, the tree dies of carbon starvation.

Finally, tree death may be caused by treefalls (term d_{treefall} in Eq. 22). To simulate this process, we first define a stochastic threshold Θ. If tree height exceeds Θ, then the tree falls with a probability equal to $1 - \Theta/h$ (Chave 1999). The parameter Θ is computed for each tree as follows:

$$\Theta = h_{\max} \times (1 - v_{\mathrm{T}} \times |\zeta|) \tag{26}$$

where $h_{\max}$ is the species-specific maximal tree height, v_{T} is a variance term (here set at 0.05), $|\zeta|$ is the absolute value of a random Gaussian variable with zero mean and unit standard deviation. The orientation of tree falls is random. Trees on the trajectory of the falling tree can be damaged, especially if they are smaller than the fallen tree (van der Meer and Bongers 1996). To model this effect, an individual variable *hurt* is defined. If a tree is within the trajectory of a treefall, its variable *hurt* is incremented by h and $\frac{h-\mathrm{CR}}{2}$ respectively, where h and CR are the tree height and crown radius of the fallen tree. If a tree height is lower than its *hurt* value, its death probability is set to $1 - \frac{1}{2}\frac{h}{hurt}$. The *hurt* variable is reset to zero at each timestep.

Seed production, dispersal and recruitment

On each 1×1 m ground site, a "seed" bank is defined, which is fed by (1) the seeds produced and dispersed from neighboring mature trees and (2) an external seed rain. In this version of the model, we assumed that a large old-growth forest surrounds the simulated stand. Given the size of the simulated area, external seed rain exceeded the local seed rain and there was no recruitment limitation by the seed bank. The seed bank was emptied at the end of each timestep. In the simulations, we did not vary the relative contribution of local seed dispersal vs. seed rain (Price et al. 2001, Lischke and Löffler 2006). The effect of species-specific dispersal limitation will be explored in a future contribution.

We assumed trees become fertile above a diameter threshold that is species-specific ($\mathrm{dbh}_{\mathrm{mature}}$; Visser et al. 2016); computed from $\mathrm{dbh}_{\mathrm{thresh}}$ as follows:

$$\mathrm{dbh}_{\mathrm{mature}} = 0.5 \times \mathrm{dbh}_{\mathrm{thresh}} \tag{27}$$

This relationship is drawn from data of reproductive status of tree species in the tropical forest of Barro Colorado Island, Panama, with maximal diameter spanning a range of 0.05–2 m (see Visser et al. 2016: Fig. S9; $R^2 = 0.81$, $n = 60$ species). In the following, a seed may be interpreted as an opportunity of seedling recruitment rather than as a true seed, since not every single seed production and dispersion is modeled and the seed-to-seedling transition is implicit.

At each timestep, each mature tree has a probability of producing seeds. The number of reproduction opportunities per timestep and per mature tree is denoted n_s. It is assumed fixed and equal for all species (here set at 10). This assumption is predicated on the fact that there is a trade-off between seed number and seed size, itself related to survival and recruitment probability. Thus the probability of germination does not depend strongly on seed size or number of produced seeds and can be assumed a zero-sum game (Coomes and Grubb 2003, Moles et al. 2004, Moles and Westoby 2006). Irregular seed production, such as mast fruiting, is a frequent reproductive strategy in tropical woody species (Norden et al. 2007), but this is not considered in this version of the model. Each of these n_s events is scattered away from the tree at a distance randomly drawn from a Gaussian distribution.

In addition, we consider n_{ext} events due to seeds immigrating from the outside. These are calculated as follows:

$$n_{ext} = N_{tot} \times f_{reg} \times n_{ha} \quad (28)$$

where N_{tot} is the total number of reproduction opportunities per hectare coming from outside (here set at 5 per m^2, to ensure saturation of the seed bank), f_{reg} the species frequency in the seed rain (here assumed constant across species), and n_{ha} the number of hectares of the simulated plot. These reproduction opportunities are uniformly distributed within the plots.

A recruitment event takes place if ground-level light availability is sufficient, i.e., above a species-specific light compensation point (LCP, which is set equal to R_{leaf}/ϕ). If several species are competing for recruitment, one of the species is picked at random as the winner out of the available species, as in a classic lottery model (Chesson and Warner 1981). Negative density dependence was also implemented at seedling recruitment stage. For seed/seedlings in the bank, and for each empty site i, we defined $p_{i,s}$ the probability of species s to establish, given that a seed of this species is present. This probability decreases with $NDD_{i,s}$ as follows:

$$p_{i,s} \propto \frac{1}{1 + \Delta_r \times NDD_{i,s}} \quad (29)$$

where Δ_r is a parameter that determines the strength of negative density dependence at the recruitment stage. If $\Delta_r = 0$ this model is equivalent to the lottery model.

Each newly recruited tree has initial size variable values, which we assume to be identical across species (dbh = 0.01 m, h = 1 m, CR = 0.5 m, CD = 0.3 m, LD = 0.8 m^2/m^3).

Parameterization, Validation Data, and Tests

Study sites and calibration/validation data

The TROLL simulator was parameterized for an Amazonian forest of French Guiana. Forests of the Guiana Shield cover some 30% of Amazonia (~1.6 million km^2), grow on Precambrian crystalline substrates (Quesada et al. 2010), and are known to have a distinct species composition (ter Steege et al. 2006), a high biomass, a low mortality rate (Johnson et al. 2016), and a tall canopy (Feldpausch et al. 2011) compared with western Amazonian forests. The study area receives ~3,000 mm/yr rainfall, with significant seasonal and interannual variation due to the movement of the Inter-Tropical Convergence Zone. A long wet season lasts from December to July, often interrupted by a short dry period in March. The dry season lasts from the end of August to November with 2–3 months with precipitation <100 mm/month (Bongers et al. 2001). Air relative humidity is typically lower and temperature higher during the dry season due to low cloud coverage.

All input data were obtained from two research stations located in primary forest. The Nouragues Ecological Research Station is located 120 km south of Cayenne within an undisturbed forest, ~50 km from Cacao, the closest village (4°05′ N, 52°40′ W; Bongers et al. 2001). The Paracou Research Station is located close to the village of Sinnamary and 20 km from the coast (5°15′ N, 52°55′ W; Gourlet-Fleury et al. 2004). Meteorological input data (PPFD, T, and relative humidity [RH]) were obtained from half-hourly measurements (SR11, Hukseflux, Delft, Netherlands; HMP155A, Vaisala, Vantaa, Finland), logged in an open area at the Nouragues Ecological Research Station, from January to December 2014. In 2014, rainfall displayed a pattern typical of the long-term trends at this site. Half-hourly VPD was deduced from relative humidity and temperature using known formulas (Monteith and Unsworth 2008). In this contribution, the same climate inputs were used every year throughout the simulations, resulting in a stable and periodic climate.

Species-specific parameters of TROLL were obtained for 163 species (Table 1). The allometric parameters were derived from ground data (Réjou-Méchain et al. 2015). Functional traits (LMA, wood density, leaf nutrient concentrations) were obtained from a trait database gathered in French Guiana (Baraloto et al. 2010). The species included in this study represent about 70% of the trees >10 cm dbh recorded in permanent plot censuses. Palms were excluded from the model simulations. All other general parameters were either measured at our sites or drawn from the literature (see Table 2).

Model outputs were compared against tree density, basal area, aboveground biomass, tree dbh distribution, species rank-abundance distribution, and tree trait distributions of mature undisturbed forest plots. Specifically, we used data from the 25-ha Paracou plot and 22 ha of plots at the Nouragues Station. In both plots, all trees ≥10 cm were located, identified to the species, and measured at least every five years since the early 1990s (Chave et al. 2008*b*, Rutishauser et al. 2010). Empirical gross primary productivity for mature forest were estimated from measurements from an eddy-flux tower located in the Paracou research station (Guyaflux; Bonal et al. 2008, Malhi 2012). Leaf fall was validated against measurements made from litterfall trap collection at both Paracou and Nouragues research stations (Chave et al. 2010).

Short-term outputs of the simulations were validated against tree inventory data of a 25-ha stand that was clear cut in 1976 and has been left regrowing since then. The site is located south of the Sinnamary village, about 10 km west of the Paracou station (ARBOCEL plot; Larpin 1989). At this site, a 6.25-ha plot was set up by CIRAD in 1989 and it has been reinventoried every two years since then.

Simulating forest regeneration

We tested the TROLL model's ability to reproduce the successional dynamics of a tropical forest, including changes in its composition and structure. We simulated regeneration from bare soil within an area of 400 × 400 m, with a constant seed external input and during 500 yr with monthly timesteps. The parameter set chosen for this simulation was taken from literature values (Table 2), and none of the parameters, except for *m*, were fine-tuned.

We assumed that after 500 yr of regeneration, a forest should have reached maturity, in the absence of abiotic disturbances. Since we were interested in following the regeneration trajectory, no spin-up was performed. A typical simulation ran for about 90 min on a portable computer with a 1.7 GHz Intel processor.

In order to assess the variability of simulated forest properties due to stochasticity alone, we ran 100 replicates and computed the variance across runs.

Sensitivity analysis

To illustrate model behavior we explored the influence of parameters on model outputs through a sensitivity analysis. We focused our attention on key parameters whose field estimates are difficult to measure, and thus rare and/or uncertain in the literature (Courbaud et al. 2015). Specifically, we explored the model sensitivity to six global model parameters (Table 2): light extinction coefficient (k), apparent quantum yield (ϕ), stomatal conductance parameter (g_1), NPP fraction allocated to wood growth (f_{wood}), NPP fraction allocated to canopy (f_{canopy}), and maximal mortality rate (m). These parameters control the main key processes of forest dynamics in the model (light diffusion, light use efficiency and carbon assimilation, carbon allocation, mortality), and few direct measurements are available for them, leading to uncertainties in their values. Here we chose not to explore the effect of seed dispersal parameters, as this question would deserve an in-depth exploration (Caughlin et al. 2016, Arroyo-Rodríguez et al. 2017). Each parameter was drawn from a uniform distribution, with lower and upper bounds based on extreme values as reported in the literature (Table 2).

The sensitivity analysis was conducted by replicating the simulation a thousand times with values of the six parameters drawn randomly and independently for each simulation from a prior distribution. We hence followed an "all-at-time" parameter sampling strategy (Pianosi et al. 2016), without assuming any relationship among parameters. Simulations were conducted on a 32-thread cluster (8-core Intel Xeon E5-2450 at 2.10 GHz).

Model sensitivity was assessed both for early stages of regeneration dynamics and for the mature forest stage. To assess early regeneration, we computed the root-mean-square error (RMSE) of simulated aboveground biomass (AGB), number of trees ≥10 cm and ≥30 cm dbh against measured values from the regeneration plot (ARBOCEL plot), for the timesteps corresponding to census dates (n = 13). For these four outputs, RMSEs were plotted against each parameter value. For the mature forest stage, we computed the output averages over the 20 last timesteps of each simulation, and plotted these values against parameters values. A model output was said to be sensitive to a parameter if it shows a significant marginal correlation with this focal parameter. Conversely, an absence of model sensitivity with respect to one parameter is revealed by an absence of trend, even though some noise may be detected in the model outputs, owing to variation due to other parameters. Trends were detected graphically using parameter-output scatter plots (Pianosi et al. 2016). We also investigated the covariation of these simulated output averages across the 1,000 simulations, and their dependence on parameters values.

To quantify the sensitivity of the model to negative density-dependence as implemented in TROLL, we tested different intensities of negative density-dependence effect on mortality and recruitment (Δ_d, Δ_r, respectively). We tested a range of these parameter values, and fixed their ratio so that they have a similar effect on recruitment and mortality. In other words, we set the magnitude of density dependence so that $\Delta_r = 100\alpha$; $\Delta_d = \alpha$, with $\alpha \geq 0$. We compared these simulations against simulations with no effect ($\alpha = 0$). We also compared simulated communities using the Inverse Simpson Diversity index (or effective number of species; Jost 2006). We tested the prediction that negative density dependence increases biodiversity and investigated its influence on ecosystem processes. For all other simulations made in this study, we assumed no negative density dependence ($\alpha = 0$).

Role of biodiversity on ecosystem functioning

We explored the influence of the number and identity of simulated species on model productivity and aboveground biomass. To this end, we performed simulations differing in the original number of species (S = 2, 5, 10, 50, 100 species) and composition. For each diversity level S, we ran a hundred simulations, by randomly picking a combination of species each time. We then recorded the contribution of each species to the total aboveground biomass, AGB_s, and to gross primary productivity, GPP_s, where s runs among the simulated species. These values were averaged over the full last simulated year. We also conducted simulations with monospecific stands for each of the 163 species parameterized in the model and recorded the simulated total aboveground biomass $AGB_{mono,s}$ and gross primary productivity $GPP_{mono,s}$.

We then quantified the net biodiversity effect on AGB and GPP, denoted ΔAGB and ΔGPP, respectively, for each of the simulations. These net biodiversity effects are defined as the difference between the simulated values and expected value under the null hypothesis that there is no effect of biodiversity, i.e., ecosystem process Y for the mixed-species forest equals the weighted sum of that in monocultures (Loreau and Hector 2001)

$$\Delta Y = \sum_{s=1}^{N} Y_s - \sum_{s=1}^{N} w_s \times Y_{\text{mono},s} \tag{30}$$

where Y is either AGB or GPP, w_s is a weight proportional to the regional species abundance (i.e., f_{reg}, see Eq. 28) such that $\sum_s w_s = 1$. For each simulation, we partitioned the net biodiversity effect into two effects: $\Delta Y = CE_Y + SE_Y$, according to Loreau and Hector (2001). The first term is the complementarity effect (CE_Y), which results from interspecific interactions (e.g., facilitation or competition) or niche partitioning. The second term is the selection effect (SE_Y) and results from the dominance of selected species with particularly efficient traits either for biomass uptake or for carbon assimilation. We tested if species richness S had a positive effect on the net biodiversity effect, and on the complementarity and selection effects separately (one-tailed t test on ΔY, CE, and SE). We also explored these effects using a one-way ANOVA with species richness as a fixed factor. Post-hoc pairwise comparisons were investigated using a Tukey HSD test. If needed to meet the assumptions of normality, ΔY, CE_Y, and SE_Y were square-root transformed while preserving positive and negative signs (Loreau and Hector 2001, Morin et al. 2011).

Biodiversity effect on ecosystem functioning may result from the functional properties of species assemblages, partly independently to changes in species richness per se. Given a species richness S, the assemblage can present different trait statistics, and these in turn may induce selection or complementarity effects. To further interpret biodiversity effects, we computed continuous functional trait community means (FM) and functional trait community diversity indices (FD; Laliberté and Legendre 2010, Morin et al. 2011) for a set of traits for each simulation. We computed both FM and FD trait-by-trait and regressed Y, ΔY, CE_Y, and SE_Y against FM and FD across simulations. Light availability is the only resource whose limitation is explicitly modeled in this version of TROLL, so we expected that the following traits would have a major effect: traits involved in light interception efficiency, such as leaf mass per area (LMA), shade tolerance, such as the light compensation point (LCP), or light niche partitioning, such as maximal adult plant height ($h_{\max}$; Westoby 1998, Poorter et al. 2009). As wood density underlies growth potential per investment (see Eq. 15) and mortality (see Eq. 23), we also included wood density as a potential predictor of biodiversity effects. For each of these four traits and for each simulation, FM and FD were computed as the weighted sum of species traits and of the species trait distance to the trait mean, respectively (Laliberté and Legendre 2010). In both cases, we used species relative abundances as weighting factors (including individuals dbh ≥10 cm). We also used relative AGB as species weights in FM and FD, but the results were similar and were not reported here.

Results

Simulating forest regeneration

Variability was low across the one hundred simulations (Figs. 2–5). Simulated stem density of trees with a dbh ≥ 10 cm (N_{10}) displayed a sharp increase early on in the forest regeneration, followed by a sharp increase in stem density of trees with a dbh ≥ 30 cm (N_{30}). Comparison with empirical measurements in a successional plot suggests that the simulation overestimated this intermediate peak in stem density. After 500 yr of simulation, N_{10} was of 480 trees/ha (range [456, 502] trees/ha), at the lower end of empirical observations (Fig. 2A). We found a good match between simulated and observed N_{30} for mature forests (simulations: 107 [102, 112] trees/ha, Fig. 2B). Simulated aboveground biomass (AGB) increased more slowly than N_{10} and N_{30}, and had barely reached stability after 500 yr of regeneration (Fig. 2C). The simulated accumulation of AGB was slightly faster than observations at the beginning of the regeneration. The long-term simulated AGB was of 327 Mg/ha (range [313, 342] Mg/ha; Fig. 2C). This is within the range of AGB values reported for mature tropical forests worldwide (Chave et al. 2008*a*) but at the lower end of the range reported for mature forests in French Guiana ([340, 430] Mg/ha; Chave et al. 2008*b*, Rutishauser et al. 2010, Réjou-Méchain et al. 2015). Finally, community-wide mean wood density reached a plateau after 100 yr, slightly below empirical observations (Fig. 2D).

The 500-yr-old simulated forest presented structural features similar to empirical observations. Ground-level LAI reached 5.4 (range [5.3, 5.4]; Fig. 3A), at the lower

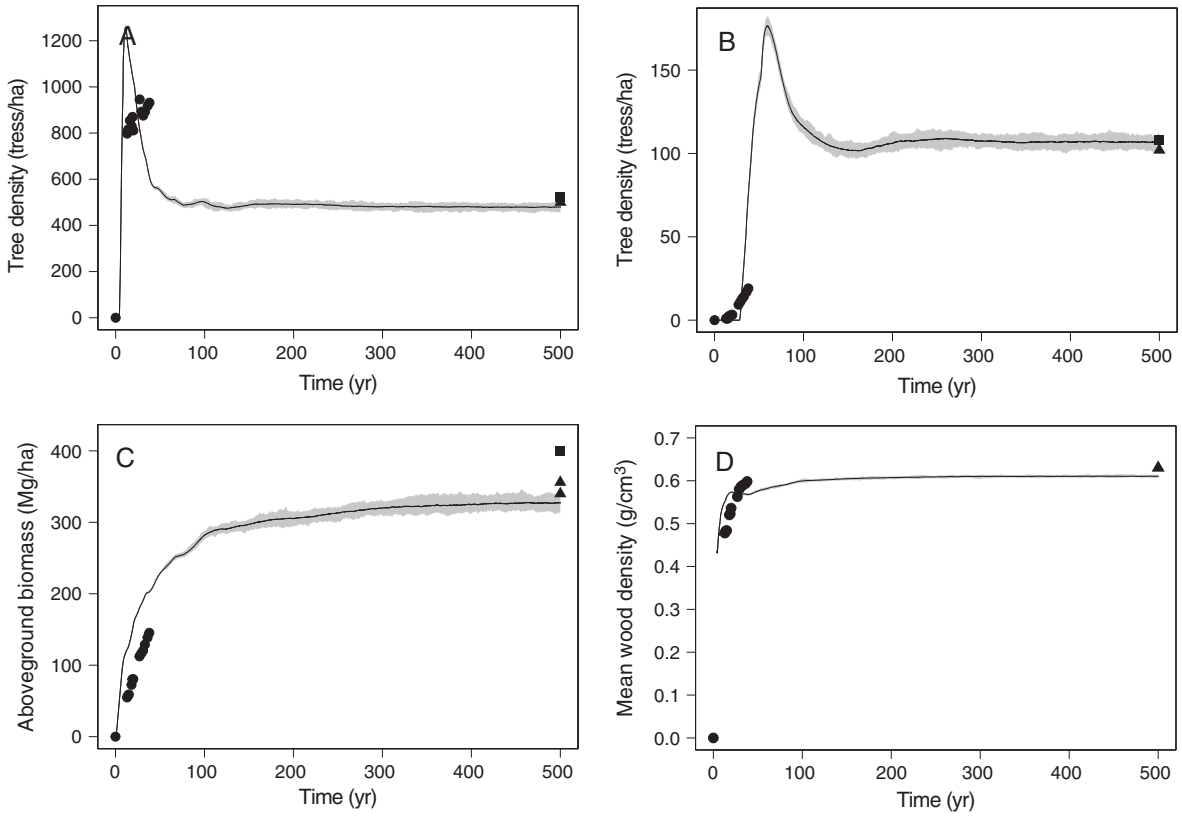

FIG. 2. Simulated forest structure, during a 500-yr-long forest regeneration, starting from bare soil, with a monthly timestep and a constant external seed rain. Dynamics of (A) stem densities of trees with a dbh $\geq$ 10 cm (in stems/ha); (B) stem densities of trees with a dbh $\geq$ 30 cm (in stems/ha); (C) aboveground biomass (in Mg/ha); and (D) mean wood density of the simulated tree community (in g/cm^3). The solid black line corresponds to the median while the shaded gray area represents the range across 100 simulations. Circle symbols correspond to the observed early-regeneration values, square and triangle symbols to the Paracou and Nouragues mature forest values, respectively.

end of the reported range for tropical forests (Clark et al. 2008), and in agreement with values reported for French Guiana (Cournac et al. 2002). Leaves were homogeneously distributed from 10 to 30 m (Fig. 3A). The diameter-size distribution was concave on a log-log plot, and the largest trees reached 150 cm dbh, in agreement with observations at our sites (Fig. 3B). The number of trees with a diameter $\leq$50 cm was slightly underestimated

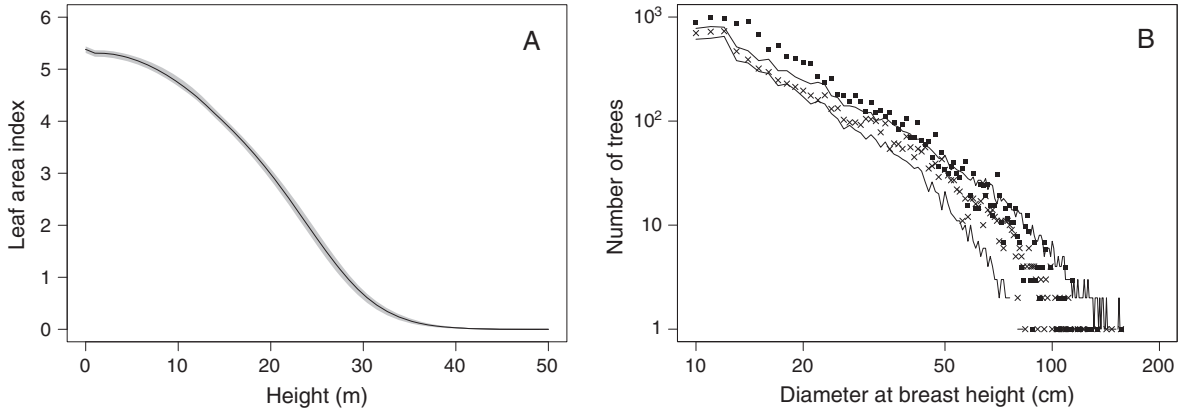

FIG. 3. Simulated mature forest (A) mean of the leaf area index as a function of height. The black line corresponds to the median while the shaded gray area represents the range across 100 simulations. (B) Size class distribution (dbh) for all trees with dbh $\geq$ 10 cm, in $\log_{10}$ scale. Crosses represent a typical simulation and the black lines represent the range envelope. Squares show the size-class distribution of the Paracou mature forest plot. Both panels were drawn for the simulated forest after 500 yr of regeneration.

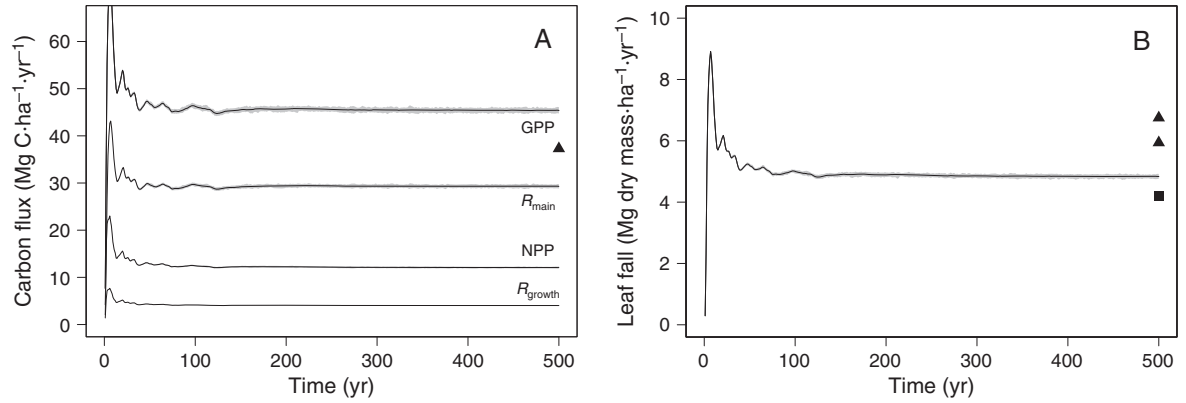

FIG. 4. Simulated carbon flux, during a 500-yr-long forest regeneration, starting from bare soil, with a monthly timestep and a constant external seed rain. (A) Dynamics of gross primary productivity (GPP) and its partitioning between net primary productivity (NPP), maintenance, and gross respiration ($R_{maintenance}$ and R_{growth}). The square corresponds to a GPP estimate from eddy-flux tower measurements at the Paracou research station (Guyaflux; Bonal et al. 2008, Malhi 2012). (B) Dynamics of leaf fall. Square and triangle symbols correspond to the Paracou and Nouragues mature forest measurements, respectively (Chave et al. 2010). In both panels, the solid black line corresponds to the median and the shaded gray area represents the range across 100 simulations.

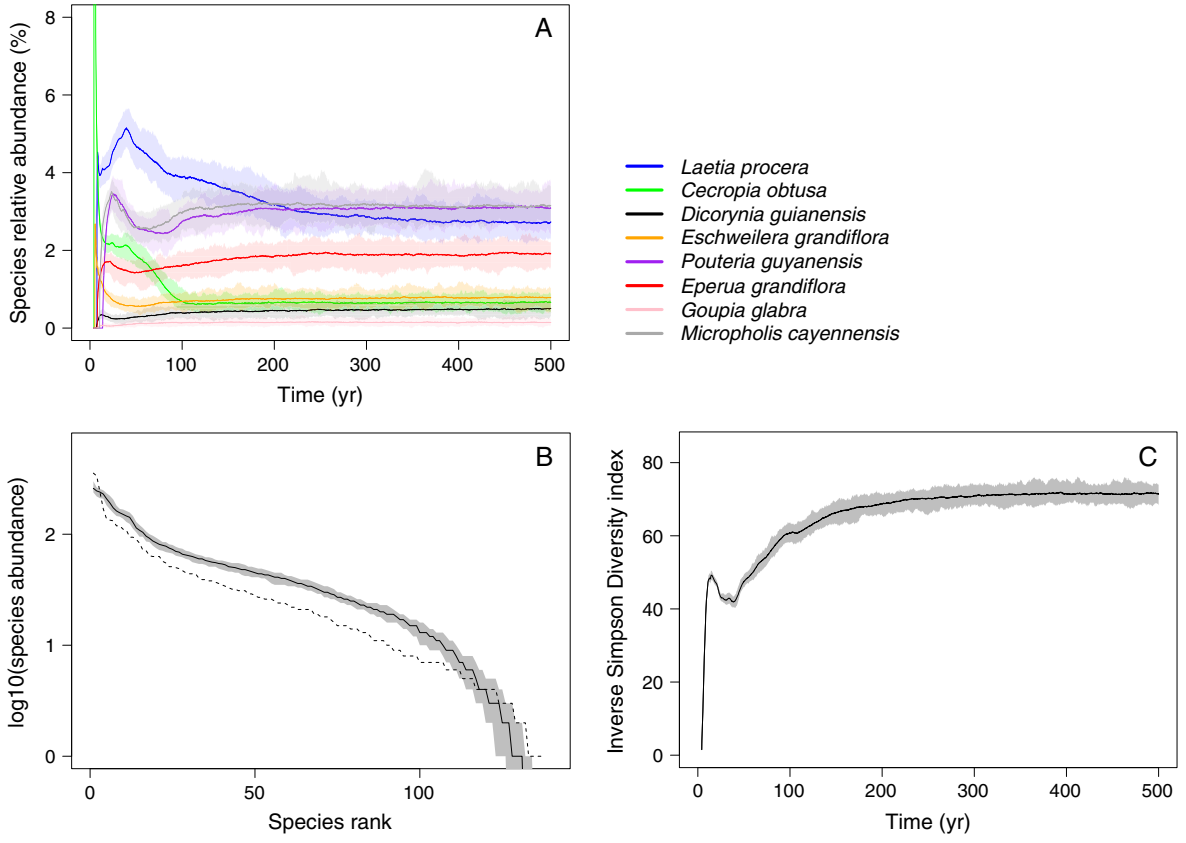

FIG. 5. Simulated tree community diversity, during a 500-yr-long forest regeneration, starting from bare soil, with a monthly timestep and a constant external seed rain. (A) Relative abundance (dbh ≥ 10 cm) trajectories during the regeneration for a subset of eight species, known to have contrasting ecology and life history. (B) Comparison between the empirical and simulated rank-abundance distributions after 500 yr of regeneration (dbh ≥ 10 cm). The dashed line represents the ranked abundances of the 139 tree species parameterized in TROLL and occurring at the Nouragues station. The solid line shows the simulated ranked abundances (median across 100 simulations) of 139 species out of the 163 simulated ones in the run. (C) Temporal change of the Inverse Simpson Diversity (ISD) index of the simulated tree community (dbh ≥ 10 cm), computed as the reciprocal of the sum of square of species relative abundances (a higher ISD means a higher diversity). The solid black lines correspond to the median and the shaded areas represent the range across 100 simulations.

in the simulations, explaining the overall relatively low simulated N_{10} at the end of the regeneration.

Gross primary productivity (GPP) stabilized within ca. 100 yr, at 45.4 Mg C·ha^{-1}·yr^{-1} (range [44.8, 46.1] Mg C·ha^{-1}·yr^{-1}), a value higher than those reported for Amazonian forests (Fig. 4A). The partitioning of GPP between autotrophic respiration and net primary productivity was in agreement with empirical studies (Bonal et al. 2008, Aragão et al. 2009, Malhi 2012). Simulated leaf fall increased sharply in the first 5 yr of the regeneration, then stabilized at 4.8 Mg C·ha^{-1}·yr^{-1} (range [4.8, 4.9] Mg C·ha^{-1}·yr^{-1}), within the range of leaf fall annual means observed empirically at our sites (Fig. 4B). The model however displayed less seasonal variability than observed empirically (Chave et al. 2008*b*, 2010).

Simulated species relative abundances presented a clear shift in community composition during the ecological succession (Fig. 5A), as is typically observed during natural secondary rainforest regeneration (Feldpausch et al. 2007, Chazdon et al. 2010, Lasky et al. 2014). Pioneer species, like *Cecropia obtusa* Trécul (Urticaceae) or *Laetia procera* (Poepp.) Eichler (Salicaceae), with fast growth rates, low wood density, and high mortality rates, dominated the community at the early stage of the regeneration. *Laetia procera*, however, maintained a relatively high density at the end of the simulated regeneration (Fig. 5A). Later-stage successional species with higher wood density, progressively increased in dominance in the community (e.g., *Pouteria guianensis* Aubl. or *Micropholis cayennensis* T.D.Penn., both Sapotaceae). The species rank-abundance distribution after 500 yr of regeneration (Fig. 5B) displayed an L-shaped profile consistent with classic ecological patterns (Rosenzweig 1995). The inverse Simpson diversity index increased at the beginning of the regeneration and stabilized within ~100 yr (Fig. 5C). In spite of the relative consistency between observed and simulated functional trajectories and species rank-abundance distributions, the most abundant species at the end of the simulated regeneration differed from the observed ones (not shown).

At the end of the regeneration, the distribution of traits for trees with a dbh ≥ 10 cm matched the observed

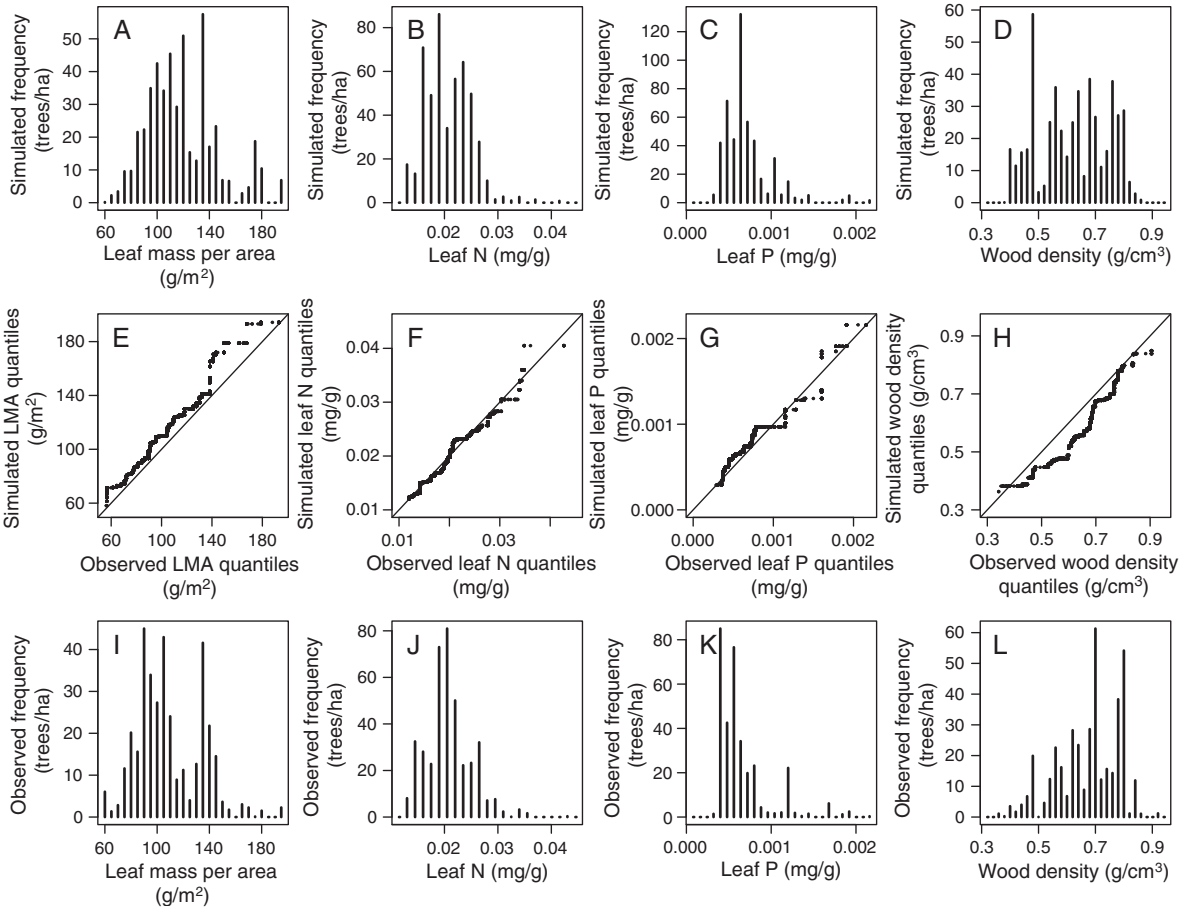

FIG. 6. Comparison of simulated and observed trait distributions for trees with dbh ≥ 10 cm in mature forests. (A–D) Trait histograms for one simulation after 500 yr of regeneration, with frequency in stems/ha; (I–L) trait histograms for the Paracou mature forest plot, with frequency in stems/ha; (E–H) QQ-plots between the corresponding simulated and observed distributions. (A, E, I) Leaf mass per area (LMA); (B, F, C) leaf nitrogen concentration; (C, G, K) leaf phosphorous concentration; (D, L, H) wood specific gravity.

distributions (Fig. 6). Simulated leaf mass per area (LMA) displayed a weak bimodal distribution, as in the observations (Fig. 6A, E, I). Simulated leaf N and leaf P were right skewed, also consistent with observations (Fig. 6B, C, F, G, J, K). The simulated wood density distribution was less left skewed than the observed one (Fig. 6D, H, L), and the simulated community-mean wood density was thus slightly lower than observed (Fig. 2D).

Sensitivity analysis

To assess the robustness and identify the main drivers of our results, we performed a sensitivity analysis on five of the global parameters, k, ϕ, f_{wood}, f_{canopy}, and m. These parameters strongly influenced almost all outputs either of the mature forest stage (Fig. 7) or of the early regeneration phase (Fig. 8). We also tested the model sensitivity to the parameter g_1; we found that it did not have a significant influence on the simulation results within the empirical ranges reported for this parameter (Lin et al. 2015).

A larger ϕ value and a smaller k value resulted in a larger GPP, AGB, and LAI (Fig. 7), and in an increase of stem density and AGB at the early stage of regeneration (higher RMSE values, Fig. 8). The ratio k/ϕ had the strongest effect of all tested parameters (Fig. 7). This ratio k/ϕ tightly constrained the whole process of light diffusion, absorption and conversion into assimilated carbon.

Allocation parameters also had a notable influence on the simulated results. A larger fraction of NPP allocated to wood (f_{wood}) resulted in a higher AGB, increasing the number of large trees at the expense of smaller ones (Figs. 7 and 8), while a larger allocation to canopy (f_{canopy}) resulted in a higher LAI (Fig. 7). The parameter m, which controls the background stem mortality rates, had a strong effect on stem density and size. Smaller values of m resulted in a higher density of large trees and less smaller trees. As a result, it strongly impacted AGB, but had a limited impact on GPP (Fig. 7).

GPP and AGB were positively but weakly correlated across the simulations (Fig. 9). The slope of this relationship was strongly controlled by m and f_{wood} (Fig. 9B, C), whereas the k/ϕ ratio determined the values of the simulated GPP and AGB along these slopes

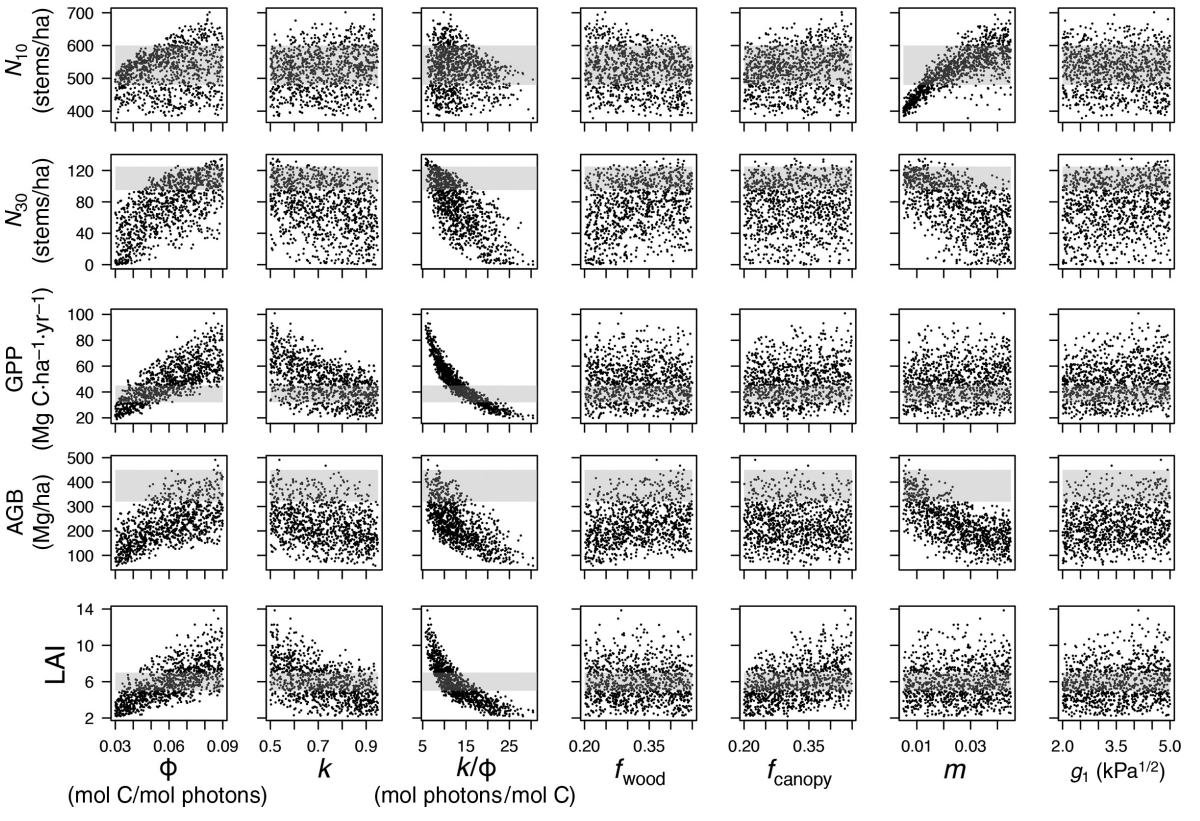

FIG. 7. Influence of parameter variation on mature forest characteristics simulated by TROLL, as revealed by a sensitivity analysis (1,000 independent simulations) varying six parameter values (ϕ, k, f_{wood}, f_{canopy}, m, and g_1) randomly and independently (Table 2). Each point corresponds to one 500-yr simulation (with monthly timestep), and outputs were averaged over the 20 last iterations. Outputs are plotted on the y-axis, with stem densities of trees with dbh $\geq$ 10 cm (N_{10}); stem densities of trees with dbh $\geq$ 30 cm (N_{30}); gross primary productivity (GPP); aboveground biomass (AGB); and leaf area index (LAI). Parameter values are plotted on the x-axis, with apparent quantum yield for carbon fixation (ϕ); light extinction coefficient (k); k/ϕ ratio; fraction of NPP allocated to wood growth (f_{wood}); fraction of NPP allocated to canopy (f_{canopy}); maximal basal mortality rate (m); stomatal conductance parameter (g_1). Gray bands indicate ranges of realistic output values, as revealed by empirical studies.

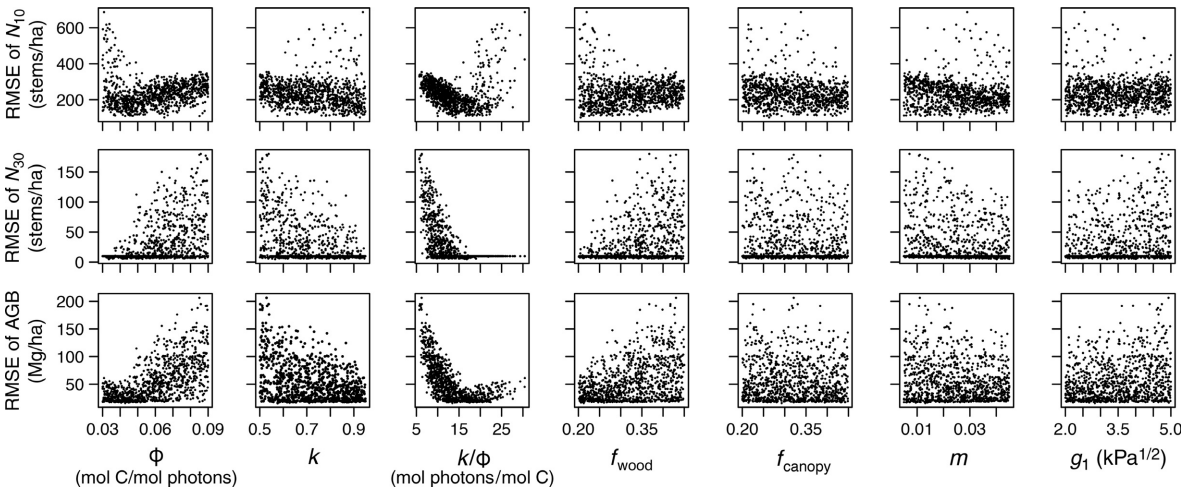

FIG. 8. Influence of parameter variation on early regeneration dynamics simulated by TROLL, as revealed by a sensitivity analysis as in Fig. 7. Each point corresponds to one 500-yr simulation (with monthly timestep), showing the root-mean-square errors (RMSE) of outputs with the corresponding values observed in a secondary forest inventory. Output RMSE are plotted on the *y*-axis, with RMSE of stem densities of trees with dbh ≥ 10 cm (N_{10}); RMSE of stem densities of trees with dbh ≥ 30 cm (N_{30}); RMSE of aboveground biomass (AGB). Parameter values are plotted on the *x*-axis, with apparent quantum yield for carbon fixation (ϕ); light extinction coefficient (k); k/ϕ ratio; fraction of NPP allocated to wood growth (f_{wood}); fraction of NPP allocated to canopy (f_{canopy}); maximal basal mortality rate (m); stomatal conductance parameter (g_1).

(Fig. 9A). A lower m or a larger f_{wood} resulted in a larger AGB increment for a given increase in productivity (Fig. 9B, C). GPP and LAI were tightly and linearly correlated, both decreasing with k/ϕ (Fig. 9E). Shifts in allocation to canopy explained the most part of the scatter in the linear relationships, a higher f_{canopy} resulting in a larger LAI for a given GPP (Fig. 9H). An increase in N_{30} led to an increase in AGB until ca. 300 Mg/ha, above which N_{30} saturated while AGB kept increasing (Fig. 9I, J). N_{10} and N_{30} were overall negatively related. A lower m value led to both a higher N_{30} and a smaller N_{10} (Fig. 9N), whereas a lower k/ϕ led to a higher N_{30} for a given N_{10} (Fig. 9M). Across the simulations, the simulated forest basal area was tightly correlated with AGB and NPP was also tightly correlated to GPP (Appendix S3), so they are not reported here.

When we simulated negative density-dependence in the model we observed an increase of the Inverse Simpson Diversity index. This increase was of 23–32% for trees with dbh ≥ 10 cm for an increasing magnitude of density dependence (α in [0.5, 2]) relative to the control ($\alpha = 0$, Fig. 10). The dominant species declined in relative abundance from 3.35% ($\alpha = 0$) to 2.45% ($\alpha = 2$; Fig. 10). Negative density dependence did not significantly affect ecosystem processes, with simulated GPP and AGB with negative density dependence staying within the range of outputs obtained without negative density dependence.

Biodiversity and ecosystem function

To illustrate the potential of this model in addressing ecological hypotheses, we tested the effect of varying biodiversity on simulated GPP and AGB by changing the simulated species richness and composition. The median GPP slightly increased with species richness, but this effect progressively leveled off above 10 species, and it was most variable across simulations for assemblages with low numbers of species (Fig. 11A). Long-term average GPP was 7.5–60.5 Mg C·ha^{-1}·yr^{-1} in single-species runs, and 29.8–59.0 Mg C·ha^{-1}·yr^{-1} in two-species runs. Thus, in some cases, we observed overyielding in comparison to simulations with 100 species and 163 species (Figs. 4A and 11A). The net biodiversity effect on GPP (ΔGPP) was significantly positive, but species richness explained only 18% of ΔGPP (Fig. 11B, Table 3). The selection effect (SE_{GPP}) was also significantly positive (all $P < 0.001$, Fig. 11C). In contrast, the complementarity effect (CE_{GPP}) was much lower in magnitude, although significantly positive at high species diversity ($S = 50$ and 100; Fig. 11D). Thus, ΔGPP was predominantly driven by the selection effect SE_{GPP}. The linear regression between ΔGPP and SE_{GPP} was strong ($P < 10^{-15}$, $R^2 = 0.99$), with the slope not significantly different from 1 and the intercept not significantly different from zero.

The influence of species richness on AGB was less clear than on GPP, with a strong variability across simulations (Fig. 11E, Table 3). Both net biodiversity effect on AGB (ΔAGB) and complementarity effect (CE_{AGB}) were weakly but significantly positive (Fig. 11F–H), but the selection effect (SE_{AGB}) was not, except for SE_{AGB} with two species (Fig. 11G). However CE_{AGB} clearly increased with species richness (Fig. 11H).

The GPP of monocultures (GPP_{mono}) was positively related with LMA ($P < 10^{-15}$, $R^2 = 0.60$) and LCP ($P < 10^{-15}$, $R^2 = 0.68$), but not to h_{max} and wood density (both $P > 0.2$). Similarly, GPP of multispecific simulations was strongly positively correlated with FM_{LMA} and FM_{LCP}, and to a lower extent with FD_{LMA} and

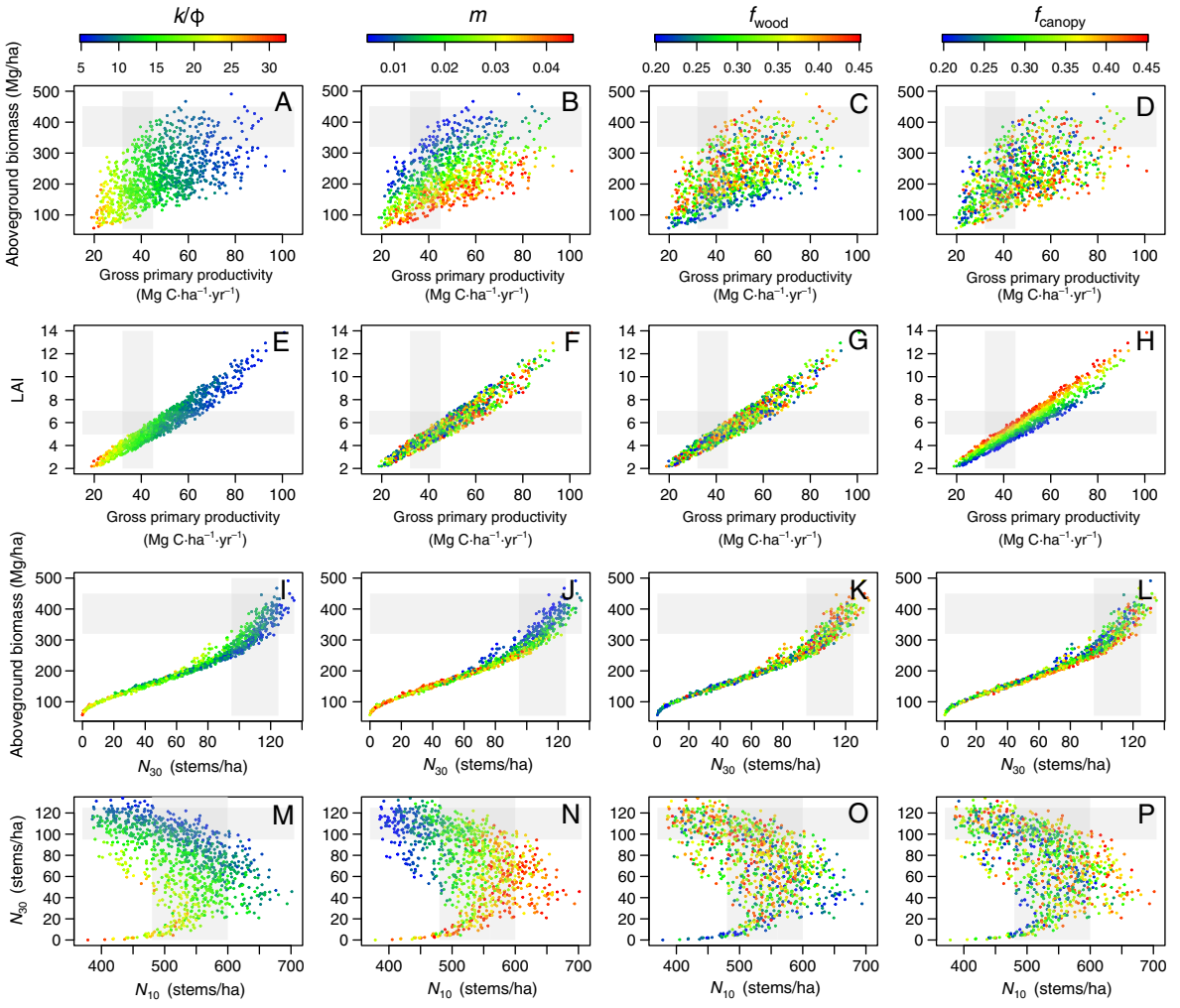

FIG. 9. Covariation of simulated forest characteristics and their dependence on parameter values, as revealed by a sensitivity analysis as in Fig. 7. Each point corresponds to one 500-yr simulation (with monthly timestep), with the outputs averaged over the 20 last iterations. (A–D) Aboveground biomass (AGB) as a function of gross primary productivity (GPP); (E–H) leaf area index (LAI) as a function of GPP; (I–L) AGB as a function of stem density of trees with dbh ≥ 30 cm (N_{30}); (M–P) N_{30} as a function of stem density of trees with dbh ≥ 10 cm (N_{10}). Panels A, E, I, and M show the covariation dependence on k/ϕ values; panels B, F, J, and N, show the covariation dependence on m; panels C, G, K, and O on f_{wood}; and panels D, H, L, and P on f_{canopy}. Gray bands indicate ranges of realistic output values, as revealed by empirical studies.

FD_{LCP} (Table 3). The AGB of monocultures (AGB_{mono}) was explained by all four investigated traits (all $P < 10^{-8}$, R^2 ranging from 0.19 to 0.52). In multispecific simulations, AGB was primarily correlated with FM_{wsg} ($P < 10^{-15}$, $R^2 = 0.39$), and with FM_{hmax} ($P < 10^{-15}$, $R^2 = 0.40$, Table 3). Trait diversity did not strongly influence AGB in multispecific simulations (Table 3). Overall, biodiversity effects on GPP and AGB were weakly explained by trait means and trait diversity, except CE_{AGB}, that was strongly correlated with FD_{hmax} ($P < 10^{-15}$, $R^2 = 0.34$, Table 3).

DISCUSSION

We described an individual-based vegetation model parameterized for a tropical rainforest of Amazonia. We then simulated the successional dynamics of the forest, and compared results with empirical data. We also performed a sensitivity analysis on key model parameters to explore the robustness of our predictions, but also to explore the drivers of ecosystem processes, structure, and composition, given environmental conditions. Finally, we used a unique feature of this model, the ability to parameterize many species within the same community, to investigate the effects of both species and functional diversities on simulated ecosystem processes. Here, we discuss the implications of our findings.

Successional dynamics

Norden et al. (2015) emphasized the idiosyncratic nature of forest regeneration in the Neotropics, and predicted

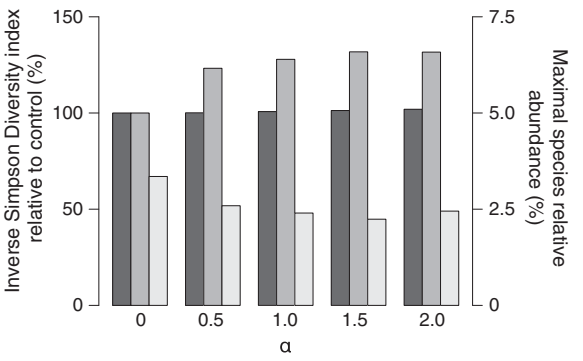

FIG. 10. Influence of simulated biotic negative density dependence processes on community composition for different magnitudes of density-dependent processes (quantified by α, see *Parameterization, validation data, and tests*). The Inverse Simpson Diversity index for trees with dbh < 10 cm (black) and dbh ≥ 10 cm (dark gray) relative to control (α = 0; left axis); and relative abundance of the most abundant species in the community (dbh > 10 cm; right axis, light gray).

that stochasticity may be as important as determinism in forest regeneration. We used TROLL to explore this question. The regeneration dynamics as simulated by TROLL were comparable to empirical observations for stem numbers, aboveground biomass, and productivity. In terms of community diversity, we found that species evenness increased as succession progressed, as observed empirically (Letcher and Chazdon 2009, Norden et al. 2009, Letcher et al. 2012, Lohbeck et al. 2014). The data–model consistency, and the low variability due to demographic stochasticity across runs, both suggest that the simulated forest succession is primarily conditioned by the proximity to mature forests and the variability of effective dispersal (Norden et al. 2009). In the future, TROLL could be used to explore this question, and to quantify the influence of the spatial structure of the seed rain on the early stages of the assembly of a regenerating rain forest (Price et al. 2001, Köhler et al. 2003, Lischke et al. 2006). We predict that the relative role of stochasticity in forest regeneration will be conditioned by the intensity of the seed rain and its species composition (Chazdon 2003, Caughlin et al. 2016, Arroyo-Rodríguez et al. 2017). Also, assigning species-specific parameters, such as seed size and dispersal distance, should help better capture the identity of dominant species, but also better quantify species-specific rates of plant migration (Lischke and Löffler 2006, Snell et al. 2014, Visser et al. 2016).

The recovery dynamics of AGB was slow (Saldarriaga et al. 1988), and associated with a shift in composition, fast-growing and low wood density species being progressively replaced by slow-growing and higher wood density species (Rozendaal and Chazdon 2015). The slower growth and larger size of late-successional species induced an increase in AGB even after a stabilization of community-wide mean wood density. This suggests that even though tropical forests store AGB within the first decades of regeneration, reaching equilibrium in AGB takes typically several centuries. The simulated AGB recovery at 20 yr was 156 Mg/ha, comparable with a recent compilation of AGB recovery rates for Neotropical forests (mean of 122 Mg/ha; Poorter et al. 2016). AGB recovery quickly slowed down thereafter, with an additional 49 Mg/ha recovered from 20 and 40 yr. The plot reached 80% of the maximal AGB stock within 85 yr, and 90% in slightly less than 140 yr. Some 50–105 yr after the start of recovery, our simulated area still accumulated between 0.5 and 2 $Mg{\cdot}ha^{-1}{\cdot}yr^{-1}$ of AGB, within the range of AGB gains reported over Amazonia (Brienen et al. 2015). This suggests that disturbances have a long-term legacy on forest AGB stocks (Chave et al. 2008*a*), although the magnitude of this effect is difficult to quantify. It would be interesting to explore whether TROLL is able to capture the cross-site variability in AGB recovery rates, due to variation in floristic composition alone.

The recovery dynamics is also quantified by monitoring the number of trees ≥10 cm dbh. In simulations, tree abundance showed a slightly too early overshooting up to 1,200 trees/ha, followed by a leveling slightly below 500 trees/ha, both findings being consistent with field data (Feldpausch et al. 2007, Chave et al. 2008*b*, Rutishauser et al. 2010; Fig. 2). For trees ≥30 cm dbh, we also observed a slightly too rapid increased of tree density in simulations compared with empirical data. We emphasize that reproducing precisely the transient dynamics of both stem density and AGB during early ecological succession is a difficult challenge because it is likely to be affected by a number of factors not modeled here, such as soil compaction, nutrient availability, pioneer species physiology, and microclimatology. Field-derived data also come with uncertainties, and the first stage of forest regeneration often displays great variability across neighboring plots (Feldpausch et al. 2007). But even though TROLL is unable to capture the precise forest regeneration dynamics, our results suggest that the processes included in the present version of the model capture much of the temporal pattern.

The shape of the simulated tree dbh size distribution was similar to that commonly reported for tropical rainforests worldwide, almost linear on a log-log plot, although markedly concave. Using an analytically tractable model, Farrior et al. (2016) proposed that this conserved pattern results from gap disturbances and the asymmetrical competition for light between canopy trees in full sunlight and understory trees in the shade (Espírito-Santo et al. 2014). In Farrior et al. (2016)'s model, the crown-area–diameter allometric relationship of understory trees drives the scaling exponent of the power law. TROLL also includes canopy disturbances and the strong dependence of tree growth rates on light availability (Eqs. 10 and 15). The slope of the simulated dbh size distribution deviates slightly from observations (Fig. 3B). To resolve this mismatch, alternative crown shape allometry could be explored (Eqs. 19–20; Jucker et al. 2017), or we could seek to improve the model fit

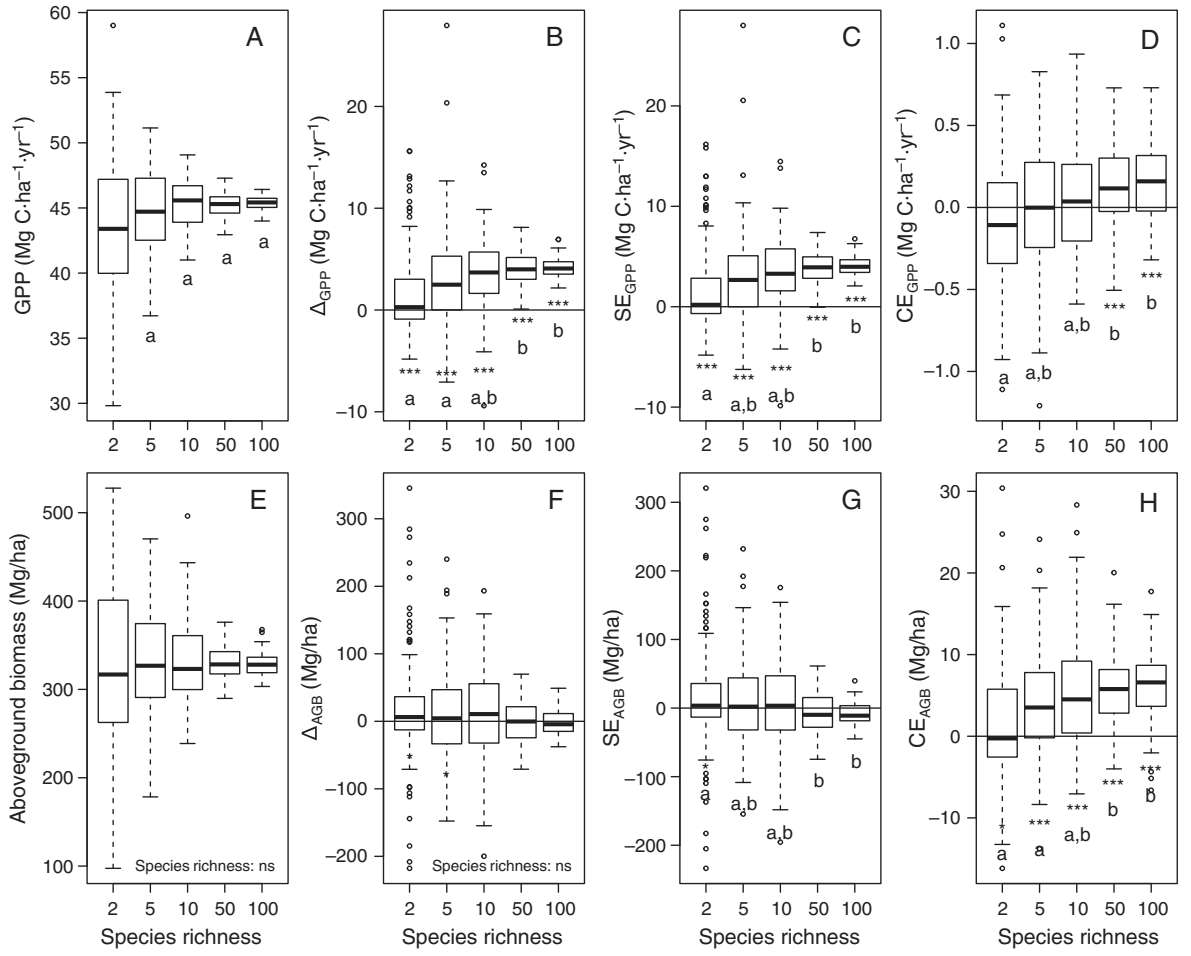

FIG. 11. Influence of species richness on (A) simulated gross primary productivity and (E) aboveground biomass, as well as on the biodiversity effects on both ecosystem properties (B, ΔGPP; F, ΔAGB) and their partitioning between selection effect (C, SE_{GPP}; G, SE_{AGB}) and complementarity effect (D, CE_{GPP}; H, CE_{AGB}). For each level of species richness (N = 2, 5, 10, 100), box plot of values (mid line, median; box edges, first and third quartiles; whiskers, lowest and highest values within 1.5 interquartile range units from the box; points, outliers outside of this range) of 100 simulations with randomly drawn species combinations among the 163 simulated species. Note the different y-axis scales. Horizontal black lines on biodiversity effect plots are the reference. Asterisks indicate mean values significantly higher from zero (one-tailed t tests; *P < 0.05, **P < 0.01, ***P < 0.001). In case of an overall effect of species richness (ANOVA; otherwise, ns), different lowercase letters indicate a significant difference between species richness levels (post hoc Tukey HSD test, P < 0.05).

by optimizing the light transmission and use efficiency parameters (k, ϕ).

Carbon assimilation and allocation were also modeled explicitly. Consistent with empirical observations, carbon fluxes stabilized within the first decade of simulation (Fig. 4). Constraining the GPP estimates of models for tropical forests is a difficult challenge (Beer et al. 2010, Jung et al. 2011), and the estimates reported here are within the range of variability reported in recent overviews (Malhi et al. 2011, 2015). The increase in GPP early on in the succession was strongly correlated with that of LAI. This appears intuitive, but unfortunately in situ measurements of GPP across chronosequences of regenerating tropical forests are currently missing. Even if the simulated LAI was consistent with observations, TROLL did not reproduce the strong seasonal pattern in leaf fall dynamics, as observed in Amazonia (Chave et al. 2010, Wu et al. 2016). This partly reflects our limited knowledge on the mechanisms underpinning seasonal shifts in leaf fall (Fu et al. 2014).

Sensitivity analysis

In order to explore the model behavior and its robustness, we assessed the implications of varying some of the model parameters across their reported range of variability. The parameters we selected control the main processes of the simulated forest, and are difficult to measure empirically. We included two parameters of light diffusion and uptake, k and ϕ, two parameters of carbon allocation, f_{wood} and f_{canopy}, and the basal mortality rate, m. These parameters were assumed invariant

TABLE 3. Biodiversity and ecosystem functioning.

	GPP				AGB			
Parameter	GPP	ΔGPP	CE_{GPP}	SE_{GPP}	AGB	ΔAGB	CE_{AGB}	SE_{AGB}
Species richness	0.07***	0.18***	0.07***	**0.16***	ns	ns	0.07***	0.03*
Functional mean (FM)								
LMA	**0.53***	0.07***	ns	0.06***	0.05***	ns	ns	ns
LCP	**0.73***	0.06***	ns	0.05***	0.02**	ns	ns	ns
h_{max}	0.01*	ns	ns	ns	**0.40***	ns	0.01**	ns
wsg	ns	ns	0.06***	ns	**0.39***	**0.10***	ns	**0.10***
Functional diversity (FD)								
LMA	0.09***	0.05***	0.01**	0.05***	0.01*	0.02**	0.06***	0.02***
LCP	**0.16***	0.07***	0.02***	0.05***	0.01**	ns	0.05***	ns
h_{max}	ns	0.01*	0.01*	0.01*	0.09***	0.03***	**0.34***	0.01*
wsg	0.02**	0.03***	0.09***	0.02**	0.03***	0.03***	0.03***	0.04***

Notes: Effect of species richness, community functional trait mean (FM), and diversity (FD) on simulated gross primary productivity (GPP) and aboveground biomass (AGB), and the biodiversity effects on GPP and AGB (ΔGPP and ΔAGB). Results were obtained from 500 simulations varying in species richness and composition, with randomly drawn combinations of N = 2, 5, 10, 50, and 100 species from 163. ΔGPP and ΔAGB are defined as the difference between the simulated values and expected values under the null hypothesis that there is no effect of biodiversity. These effects are partitioned into a complementarity effect (CE_Y, with Y = AGB or GPP), which results from interspecific interactions or niche partitioning, and a selection effect (SE_Y), which results from the dominance of selected species with particularly efficient traits either for biomass uptake or for carbon assimilation. Test of species richness effect: one-way ANOVA with species richness as a fixed factor. Test of FM and FD effects: linear regression with FM and FD as independent variables. Four species-specific traits are explored: leaf mass per area, LMA; light compensation point, LCP; maximal adult plant height, h_{max}; and wood specific gravity, wsg. For each trait and each simulation, FM and FD were computed as the weighted sum of species traits and of the species trait distance to the trait mean, respectively. In both cases, we used species relative abundance as weighting factors (including individuals dbh ≥ 10 cm). Values are R^2 of models (n = 500 simulations); R^2 above 0.10 are shown in boldface type.
*P < 0.05; **P < 0.01; ***P < 0.001; ns, non-significant.

across species and independent of environmental conditions, because a more detailed parameterization is lacking for them. Even though these parameters are common in vegetation models, they are usually assumed rather than parameterized. However, it is known that the light extinction factor k varies with leaf angle, which depends on both environment and species (Meir et al. 2000, Kitajima et al. 2005). Likewise, the apparent quantum yield ϕ is expected to vary with leaf thickness and leaf light exposure (Long et al. 1993, Poorter et al. 1995). Mortality rate and allocation patterns vary among species strategies and local environments, resulting in different tree architectures and resource acquisition (Iida et al. 2011, 2012). Within the range of parameter values, our simulations always included empirically realistic values of summary statistics such as AGB, LAI, GPP, N_{10}, and N_{30} at the end of the simulation (+500 yr; Fig. 7). In our simulations, the model sensitivity to parameters is in agreement with our assumptions and with comparable existing modeling studies (Medlyn et al. 2005, Mercado et al. 2009*b*).

Fine-tuning of the parameters to optimize the representation of the processes was not a goal in this study. With highly parameterized models such as ours, it is important to carefully explore the model behavior before implementing such optimization procedures, and this is why we did not attempt to fine-tune the model parameters. Inverse-modelling approaches hold great promise to calibrate parameters for complex models such as forest growth simulators (e.g., approximate Bayesian computation; Hartig et al. 2012, 2014, Lagarrigues et al. 2015, Courbaud et al. 2015). However, the risk that the model shows an equally good fit with very different model combinations should be considered. This equifinality problem can only be minimized in practice by improving the quality of the parameter priors.

The sensitivity analysis showed that modeled GPP and AGB were not strongly correlated. Lower species stem mortality rates (m) or increased allocation of productivity to wood growth (f_{wood}) led to a larger AGB stock for a given GPP (Fig. 9B, C). Multiple processes shape the pathway of assimilated carbon by photosynthesis toward standing living biomass: AGB is tightly related to NPP multiplied by residence time (defined as the inverse of death rate; Friend et al. 2014), while NPP is tightly related to GPP times allocation into tissue (Malhi et al. 2015, Johnson et al. 2016). Our simulation runs confirm that stem mortality is a strong predictor of AGB stocks (Johnson et al. 2016), as well as carbon allocation (Doughty et al. 2014, Malhi et al. 2015). The sensitivity analysis spanned the observed range of stem mortality and allocation patterns due to variation in environmental conditions, soil composition, and floristic composition across Amazonia (Quesada et al. 2010, 2012). Better empirical estimates of ecosystem-wide residence times and allocation would help constrain this type of models (Litton et al. 2007, Friend et al. 2014, Malhi et al. 2015, Johnson et al. 2016, Clark et al. 2017).

The processes of light diffusion, absorption, and the resulting carbon uptake by photosynthesis, which were constrained by the k/ϕ ratio, controlled GPP and AGB independently of stem mortality and allocation processes (Fig. 9A). Variation in light absorption across sites may explain the observed differences in the effect of stem mortality rate on AGB (Johnson et al. 2016). Also, the major predictor of GPP variation was LAI, as has been found in previous global syntheses (Beer et al. 2010, Fig. 9I). A more efficient light uptake and conversion to carbon (lower k/ϕ) allowed more dense and packed canopies to develop, with more large trees and higher LAI.

Our model of stomatal conductance is based on recent theoretical advances (Medlyn et al. 2011, Prentice et al. 2014). Considering the importance of stomatal conductance and internal CO_2 concentration in driving productivity, we expected the model to be sensitive to the main parameter g_1. The parameter g_1 relates the ratio of internal to ambient CO_2 concentration (c_i/c_a) to air vapor pressure deficit (VPD; Eq. 7). However, the model outputs presented no clear trends with g_1, although the range of g_1 values spanned the empirical range (Lin et al. 2015, Table 2). Within this range, and given the VPD and temperature amplitudes at our site, variation in carbon assimilation due to changes in g_1 is limited (see Appendix S4 for an illustration), and a more robust test of this model should be conducted, for instance at a forest–savanna transition (Domingues et al. 2010). Alternative models of stomatal conductance with different sensitivities to VPD have been found to yield similar performance for tropical evergreen forests (Knauer et al. 2015). We also tested a dependence of g_1 as a function of wood density, as suggested in Lin et al. (2015: Fig. 3). In agreement with our sensitivity analysis, this change in the model did not improve the fit to output summary statistics (results not shown).

Negative density dependence and species coexistence

In tropical ecology, it has long been established that one of the foremost processes driving the abundance of species, the maintenance of rare species, and indirectly ecosystem processes, is the so-called Janzen-Connell hypothesis (Janzen 1970, Connell 1971). Because we aimed at jointly modeling ecosystem processes and biodiversity, our sensitivity analysis also included a test of the hypothesis that negative density dependence (the competitive advantage of rare species over abundant ones) could alter community structure and also regulate plant productivity (Terborgh et al. 2001, Schmitz 2003).

We found an increase in community diversity (evenness) due to negative density dependence, an effect that increased through life stages. This result is in agreement with experimental studies and observations that negative density dependence is key to explain the large species diversity in the tropics (Wright 2002, Uriarte et al. 2004, Gonzalez et al. 2010, Bagchi et al. 2014). Modeling studies have previously suggested that negative density dependence is needed to reproduce observed biodiversity (Lischke and Löffler 2006). In our study, negative density dependence had a limited influence on community diversity since diversity was primarily maintained by immigration, but we would expect a stronger effect in situations where the external seed rain contributes less, as would occur in fragmented landscapes (Laurance et al. 1998, Laurance 2008, Ewers et al. 2017). Also, in changing climates, it is expected that environmental filtering will be stronger, which would result in drastic changes in floristic composition. This prediction is already observed and may be soon amplified (Fauset et al. 2012, Meir et al. 2015, Feldpausch et al. 2016, van der Sande et al. 2016). For these reasons, adding stabilizing diversity processes in vegetation models is an important objective.

Biodiversity and ecosystem functioning

By simulating ecosystem processes while keeping track of species identity of individuals, we could investigate the link between biodiversity and ecosystem functioning (BEF). This application illustrates the potential of TROLL to address practical and theoretical ecological questions (see also Chave 2001). BEF relationships have been intensely studied over the last decades, through experiments (Cardinale et al. 2009), observations along natural gradients of species richness (e.g., Paquette and Messier 2011, Grossiord et al. 2014) or theory (e.g., Loreau 1998, 2010). Experimental studies have often been limited in time and to low species richness. Studies have predominantly focused on grasslands and, to a lesser extent, on temperate forests (but see Potvin and Gotelli 2008, Finegan et al. 2015, Lohbeck et al. 2015, Poorter et al. 2015, Liang et al. 2016).

By virtually manipulating the number and identity of species, we assessed the effect of species richness and functional composition on the simulated gross primary productivity (GPP) and aboveground biomass (AGB) of a tropical forest plot. Species richness had a positive effect on both ecosystem characteristics, even though this effect leveled off at high species richness for GPP and was weak for AGB. These results are in line with previous observations (Grime 1997, Chisholm et al. 2013, Sullivan et al. 2017). As seen above, the contrasting effect of species richness on GPP and AGB illustrates the need to explore these ecosystem metrics separately, and not use one as a surrogate of the other (Chisholm et al. 2013).

Species richness alone explained a small fraction of the variability in GPP and AGB across simulations. We were able to simulate the influence of biodiversity at a relatively large spatial scale, and the biodiversity effect vanishes with increasing spatial scale, as found empirically in a range of tropical forests (Chisholm et al. 2013, Sullivan et al. 2017). Also, we observed a strong variability for a given species richness, showing that taxonomic composition of the tree species assemblage controls ecosystem properties more than the number of species per se.

In simulations with low species richness, we found particularly contrasted ecosystem properties. The most

direct way to assess this finding would be to contrast the ecosystem properties in old-growth mixed-species forests with that of monospecific plantations. In French Guiana, an experimental set-up of monospecific plantations has been established in the early 1980s to test the possibility of production planting for 16 local timber species (Roy et al. 2005, Bréchet et al. 2009). At this site, Bréchet et al. (2009) showed that litterfall presented a four-fold variation across the 16 monospecific plantations, and that basal area showed a 10-fold variation. Litterfall is a reasonably good proxy for NPP in tropical forests (Malhi et al. 2011), and basal area is a good proxy for AGB. This demonstrates that tropical tree species, when grown alone, do display the large range of variation in the ecosystem properties we evidenced in our simulations (see also Bauters et al. 2015).

In our simulations, the major impact of species diversity on GPP was the selection effect, the influence of a selective group of efficient species on the ecosystem, rather than a complementarity effect in resource acquisition across species niches. This finding contrasts with some empirical studies where a stronger complementarity than selection effect was evidenced (Loreau and Hector 2001), but is in agreement with empirical results in tropical forests (Bauters et al. 2015, Finegan et al. 2015, Chiang et al. 2016, Lohbeck et al. 2016, Prado-Junior et al. 2016). However, our model does not include any other resource limitation than light, especially nutrient and water limitations. Thus, our results should be interpreted as a null scenario against which to test additional processes. For instance, it would be interesting to test how the addition of a nutrient cycle would alter our conclusions, since most tropical forests are phosphorus limited (Wright et al. 2011, Barantal et al. 2012, Batterman et al. 2013). Belowground element trade among individuals of different species (Klein et al. 2016) may also induce higher complementarity effect. Also, asynchronous leaf phenology may lead to complementarity through temporal niche partitioning in tropical forests (Reich et al. 1992, Sapijanskas et al. 2014), but TROLL currently does not include this effect, and the mechanisms triggering leaf fall are complex and poorly documented.

Consistent with a stronger selection than complementarity effect, GPP and AGB were better explained by community-weighted mean functional traits than functional trait diversity (Finegan et al. 2015, Chiang et al. 2016, Prado-Junior et al. 2016). Gross primary productivity was strongly positively correlated with both leaf mass per area and light compensation point weighted means (Table 3). This result indicates that GPP increases with both leaf lifespan, itself related to LAI, and leaf productivity (Reich et al. 1992, Sterck et al. 2006, Falster et al. 2011, Prado-Junior et al. 2016). Empirical studies have yielded contrasting results, especially in early-successional forests, which could be due to the advantage of low-LMA species early on in the regeneration (Sterck et al. 2006, Lohbeck et al. 2013, 2014, Finegan et al. 2015). Similarly, AGB was positively correlated with community-weighted mean wood density, itself related to carbon residence time (see Eq. 23), and with community-weighted mean maximal height, in agreement with recent studies (Falster et al. 2011, Finegan et al. 2015, Chiang et al. 2016, Mensah et al. 2016), and with our sensitivity analyses. Also, the complementarity effect on AGB was strongly correlated to the dispersion of species maximal heights, as expected from a better canopy packing and complementarity of light niches due to heterogeneity in tree heights (Poorter et al. 2005, Sapijanskas et al. 2014). This pattern has already been described in the literature (Morin et al. 2011, Ruiz-Jaen and Potvin 2011).

Functional traits are known to vary across species and sites (Fyllas et al. 2009, Baraloto et al. 2010, Banin et al. 2012); our analysis suggests that it would be important to use site-specific traits to simulate ecosystem functioning (ter Steege et al. 2006, Quesada et al. 2012, Fyllas et al. 2014). This remains a challenge because spatial variability in trait values is still poorly represented in vegetation models (de Almeida Castanho et al. 2016, Johnson et al. 2016).

Perspectives in forest ecosystem modeling

The current version of TROLL offers several novelties over previous models of the same type. It also opens new perspectives in modeling, which we hope to address in the future. TROLL integrates several advances in plant physiology, but it also reflects the limits of this field. For example, plant respiration is less well understood than photosynthesis (Atkin et al. 2014). Allocation and mortality mechanisms are also less well known than assimilation (Malhi et al. 2015). Since it adopts a finer-grained representation of vegetation structure and diversity than most DVMs, TROLL is an efficient tool to test alternative hypotheses on these understudied processes. It could be used to test processes that may be relevant for future improvements of DVMs and assess the level of details required in model representation. It could also be helpful to propose generic scaling-up relationships (Bellassen et al. 2010). Ecosystem experiments in tropical forests, such as the new generation of FACE experiments (Norby et al. 2016), through-fall exclusion experiments (Meir et al. 2015), nutrient addition experiments (Powers et al. 2015), and other in situ experimental approaches (Fayle et al. 2015), all provide opportunities of data-model interactions and hypothesis testing on poorly known processes (Medlyn et al. 2015, 2016). TROLL should facilitate data–model comparisons, as its outputs match the scale and resolution of field measurements.

The current version of TROLL does not explicitly model the water cycle and plant hydraulics. The two-month dry season observed in French Guiana rarely results in major tree physiological stresses (Buchmann et al. 1997, Bonal et al. 2008), and this explains the relatively good fit of the model with observations. However, drier tropical areas are more water limited (Restrepo-Coupe et al. 2013, Guan et al. 2015, Wagner et al.

2016), and this situation may be more pervasive in the future as drought could become a prevailing mechanism of tropical forest vulnerability (Boisier et al. 2015, Meir et al. 2015). It would thus be important to include the water cycle to project future ecosystem states. TROLL has an appropriate model structure to include a species-level description of drought tolerance, an important point since there is a strong inter-specific variation of plant drought tolerance (Engelbrecht and Kursar 2003, Klein 2014, Maréchaux et al. 2015, Martínez-Vilalta et al. 2014). Including the water cycle in TROLL could also improve the successional dynamics since temperature and VPD are higher in clearings than in dense canopy of mature tropical forest (Marthews et al. 2008, Lebrija-Trejos et al. 2011). The strong evaporative demand in secondary forests would imply reduced carbon assimilation, which could in turn explain why our simulated forest regeneration dynamics was more rapid than empirical observations.

Carbon allocation was described empirically, assuming a fixed proportion of total NPP allocated to wood growth and foliage production, and through the use of fixed and field-derived allometric equations. This approach is similar to that developed in other forest growth models (e.g., Köhler and Huth 1998, Moorcroft et al. 2001, Fyllas et al. 2014). However, carbon allocation is a dynamic process that can vary with resource limitation, such as water and nutrients, and thus across sites (Litton et al. 2007, Chen et al. 2013, Doughty et al. 2014, Malhi et al. 2015; Appendix S5: Fig. S1). Rowland et al. (2014) demonstrated that the fitting of seasonal allocation parameters yields better match with empirical observations in a tropical forest. Scheiter and Higgins (2009) implemented an approach to ensure that the allocation to biomass pools depends on the most limiting resource (see also Friedlingstein et al. 1999, Guillemot et al. 2017), but a mechanistic understanding of plant carbon allocation is still lacking (Farrior et al. 2013, Schippers et al. 2015). One step forward would be to explicitly represent allocation of photosynthates to carbon reserves (non-structural carbohydrates, NSC; Dietze et al. 2014; Appendix S5: Fig. S1). It would be useful to add a pool of NSC because mortality due to carbon starvation (see d_{starv} in Eq. 22) could then be expressed directly in terms of NSC depletion. Fortunately, the role of such dynamic NSC storage in plant metabolism maintenance, growth control, and mortality processes is being increasingly studied (Sala et al. 2012, Körner 2015, Martínez-Vilalta et al. 2016).

More generally, closing the carbon cycle is an important challenge. Soil carbon fluxes, root exudates, and heterotrophic respiration are currently absent in TROLL, despite their known importance in the carbon cycle (e.g., Bonal et al. 2008, Davidson et al. 2011; Appendix S5: Fig. S1). A proper comparison of the model against eddy-flux data would also require closing the carbon balance (Baldocchi et al. 2001, Baldocchi 2003, Bonal et al. 2008). Adding these features would help explore the role of mycorrhizal interactions in mediating nutrient uptake in plants, but also in better understanding species complementarity on ecosystem function (Bardgett et al. 2014, Klein et al. 2016). The integration of an explicit nutrient cycle with colimitation for nitrogen and phosphorous would also be a very useful advance (Prentice et al. 2007, Fernández-Martínez et al. 2014, Powers et al. 2015; Appendix S5: Fig. S1) given the on-going alteration of nutrient availability by humans (Peñuelas et al. 2013). Overall, the integration of the water and nutrient cycles and of explicit tree NSC storage would help explore the control of nutrient and water availability on growth, and shift from a source-driven to a sink-driven carbon modeling approach (Muller et al. 2011, Fatichi et al. 2014, Körner 2015, Guillemot et al. 2017; Appendix S5: Fig. S1).

Another important, and missing, process in TROLL is herbivory. Herbivory makes a major contribution to carbon and nutrient cycles, as herbivores consume as much as ~20% of foliar production (Metcalfe et al. 2014) and they regulate tropical forest productivity (Terborgh et al. 2001). Pioneer species have been reported to suffer more from herbivory than late-successional species, with investment into leaf defense traits increasing with succession (Coley et al. 1985, Poorter et al. 2004, Lohbeck et al. 2013). Attempts have already been made to dynamically and jointly model plant dynamics and that of their predators (Harfoot et al. 2014); TROLL offers an opportunity to explicitly model the host-specificity of predators, and their individualistic response to environmental changes, and to model the joint dynamics of plants and herbivorous insects (Forister et al. 2015). To that end, manipulative experiments on whole ecosystems would prove valuable (Fayle et al. 2015).

Perspectives in forest biodiversity modeling

Tropical forests shelter thousands of co-occurring tree species (Hubbell et al. 2008) and these span a broad range of ecological and functional properties. Advances in plant functional trait research represent a major advance in understanding plant physiology and ecological functions (Kattge et al. 2011, Díaz et al. 2016). One original feature of TROLL is that it describes species individually, thus providing a finer description of biodiversity than the usual approaches based on a limited number of plant functional types, or even the descriptions based on a continuous spectrum of traits (Sakschewski et al. 2015). This level of biodiversity description was implemented in a parameterization relying on only seven species-specific functional traits (Table 1), all of which are relatively easy to measure in the field. Indeed, allometric parameters can be obtained from the observation of 10–20 individuals spanning the size range of the species, and leaf- and stem-level parameters can be measured from a limited sampling of tissue (Patiño et al. 2012). Thus, the model requirements of TROLL closely parallels current efforts of trait data collection, and for this reason it should be applicable at many tropical forests sites.

The species-level description in TROLL is similar to functional type descriptions in many DVMs. The species-specific parameters are fixed and prescribed, and are identical among the individuals of the same species. Thus, we overlook intraspecific functional variability. There is abundant evidence of the importance of intraspecific variation in ecology and evolutionary biology (Chesson 2000, Albert et al. 2011, Laughlin et al. 2012, Snell et al. 2014, Le Bec et al. 2015), and this variation may contribute to buffering the effect of climate change (e.g., Scheiter et al. 2013). However, ignoring intraspecific variation is a reasonable simplification. Since TROLL has an object-oriented code structure, the integration of intraspecific variability will be easily implemented and is an interesting avenue for future research. Also, independent of model performance, the ability of TROLL to parameterize many species in the model represents a way forward to relate empirical knowledge and ecological data sets to vegetation models.

One driving motivation behind modeling species one by one in TROLL is that each species has its peculiar evolutionary history and ecology, and should therefore be considered as the most natural unit in the description of natural communities (Gleason 1926). Recent modeling studies have followed a different route to model biodiversity. They did not explicitly model species one by one, but they used empirically documented functional trade-offs (Wright et al. 2004) to constrain individual trait associations into a biologically realistic space (Scheiter et al. 2013, Sakschewski et al. 2015). This approach is computationally efficient and less data demanding than ours, but it is predicated on varying trait combinations within strictly limited constrains, that may ignore a more complex set of constraints (Laughlin 2014, Li et al. 2015, Asner et al. 2016). TROLL is a useful model to explore the generality of this simplification and its implications for forest dynamics.

TROLL yields outputs with full taxonomic information, similar to field inventories. Correspondence between field data and model structure is desirable if we wish to take advantage of empirical knowledge and to validate models. Thus we could investigate theoretical questions such as the effect of species richness and composition on ecosystem properties. This choice also has important practical implications. Indeed, about one-half of tropical forests are designated for timber production (Blaser et al. 2011), and it is important to assess and predict the impact of logging scenarios on carbon losses and biodiversity and structure modifications. Species-level integration could inform management approaches, as logging practice crucially depends on commercial species of particular interest. In French Guiana, only two species, *Dicorynia guianensis* and *Qualea rosea,* account for up to 60% of the total timber production. TROLL could thus help assess forest vulnerability to timber exploitation (e.g., Fargeon et al. 2016) by modeling logging scenarios, selecting focal species at a reference diameter.

Acknowledgments

We thank D. Bonal, F. Bongers, P. Ciais, B. Hérault, A. Huth, G. Jaouen, E. Joetzjer, R. Pélissier, J. Penuelas, L. Sack, N. Viovy, and S. J. Wright for fruitful discussions, and P. Solbès for support. We also thank the numerous field workers involved in data collection at the permanent field research sites of French Guiana (Paracou and Nouragues) and the managing research institutes INRA, CIRAD, and CNRS, the Guyaflux tower (PI D. Bonal), and the Guyafor and Climfor projects (PI B. Hérault). This work has benefited from "*Investissement d'Avenir*" grants managed by the French Agence Nationale de la Recherche (CEBA, ref. ANR-10-LABX-25-01 and TULIP, ref. ANR-10-LABX-0041; ANAEE-France: ANR-11-INBS-0001) and from an additional ANR grant (BRIDGE project) and funds from CNRS to the Nouragues station. Computations performed on EDB-Calc Cluster, which uses a software developed by the Rocks(r) Cluster Group (San Diego Supercomputer Center, University of California, San Diego and its contributors), hosted by the laboratory "Evolution et Diversité Biologique" (EDB).

Literature Cited

Albert, C. H., F. Grassein, F. M. Schurr, G. Vieilledent, and C. Violle. 2011. When and how should intraspecific variability be considered in trait-based plant ecology? Perspectives in Plant Ecology, Evolution and Systematics 13:217–225.

Amthor, J. S. 1984. The role of maintenance respiration in plant growth. Plant, Cell & Environment 7:561–569.

Aragão, L. E. O. C., et al. 2009. Above- and below-ground net primary productivity across ten Amazonian forests on contrasting soils. Biogeosciences 6:2759–2778.

Arroyo-Rodríguez, V., F. P. L. Melo, M. Martínez-Ramos, F. Bongers, R. L. Chazdon, J. A. Meave, N. Norden, B. A. Santos, I. R. Leal, and M. Tabarelli. 2017. Multiple successional pathways in human-modified tropical landscapes: new insights from forest succession, forest fragmentation and landscape ecology research. Biological Reviews 92:326–340.

Asao, S., R. Bedoya-Arrieta, and M. G. Ryan. 2015. Variation in foliar respiration and wood CO_2 efflux rates among species and canopy layers in a wet tropical forest. Tree Physiology 35:148–159.

Asner, G. P., D. E. Knapp, C. B. Anderson, R. E. Martin, and N. Vaughn. 2016. Large-scale climatic and geophysical controls on the leaf economics spectrum. Proceedings of the National Academy of Sciences USA 113:E4043–E4051.

Atkin, O. K., J. R. Evans, M. C. Ball, H. Lambers, and T. L. Pons. 2000. Leaf respiration of snow gum in the light and dark. Interactions between temperature and irradiance. Plant Physiology 122:915–924.

Atkin, O. K., D. Bruhn, V. M. Hurry, and M. G. Tjoelker. 2005. The hot and the cold: unravelling the variable response of plant respiration to temperature. Functional Plant Biology 32:87–105.

Atkin, O. K., P. Meir, and M. H. Turnbull. 2014. Improving representation of leaf respiration in large-scale predictive climate–vegetation models. New Phytologist 202:743–748.

Atkin, O. K., et al. 2015. Global variability in leaf respiration in relation to climate, plant functional types and leaf traits. New Phytologist 206:614–636.

Bagchi, R., R. E. Gallery, S. Gripenberg, S. J. Gurr, L. Narayan, C. E. Addis, R. P. Freckleton, and O. T. Lewis. 2014. Pathogens and insect herbivores drive rainforest plant diversity and composition. Nature 506:85–88.

Baldocchi, D. D. 2003. Assessing the eddy covariance technique for evaluating carbon dioxide exchange rates of ecosystems: past, present and future. Global Change Biology 9:479–492.

Baldocchi, D., et al. 2001. FLUXNET: a new tool to study the temporal and spatial variability of ecosystem–scale carbon dioxide, water vapor, and energy flux densities. Bulletin of the American Meteorological Society 82:2415–2434.

Ball, J. T., I. E. Woodrow, and J. A. Berry. 1987. A model predicting stomatal conductance and its contribution to the control of photosynthesis under different environmental conditions. Pages 221–224 *in* J. Biggins, editor. Progress in photosynthesis research. Martinus Nijhoff Publishers, Leiden, The Netherlands.

Banin, L., et al. 2012. What controls tropical forest architecture? Testing environmental, structural and floristic drivers. Global Ecology and Biogeography 21:1179–1190.

Baraloto, C., C. E. T. Paine, S. Patiño, D. Bonal, B. Hérault, and J. Chave. 2010. Functional trait variation and sampling strategies in species-rich plant communities. Functional Ecology 24:208–216.

Barantal, S., H. Schimann, N. Fromin, and S. Hättenschwiler. 2012. Nutrient and carbon limitation on decomposition in an Amazonian moist forest. Ecosystems 15:1039–1052.

Bardgett, R. D., L. Mommer, and F. T. De Vries. 2014. Going underground: root traits as drivers of ecosystem processes. Trends in Ecology & Evolution 29:692–699.

Batterman, S. A., L. O. Hedin, M. van Breugel, J. Ransijn, D. J. Craven, and J. S. Hall. 2013. Key role of symbiotic dinitrogen fixation in tropical forest secondary succession. Nature 502:224–227.

Bauters, M., E. Ampoorter, D. Huygens, E. Kearsley, T. De Haulleville, G. Sellan, H. Verbeeck, P. Boeckx, and K. Verheyen. 2015. Functional identity explains carbon sequestration in a 77-year-old experimental tropical plantation. Ecosphere 6:1–11.

Beer, C., et al. 2010. Terrestrial gross carbon dioxide uptake: global distribution and covariation with climate. Science 329:834–838.

Bellassen, V., G. Le Maire, J. F. Dhôte, P. Ciais, and N. Viovy. 2010. Modelling forest management within a global vegetation model—Part 1: model structure and general behaviour. Ecological Modelling 221:2458–2474.

Bernacchi, C. J., C. Pimentel, and S. P. Long. 2003. In vivo temperature response functions of parameters required to model RuBP-limited photosynthesis. Plant, Cell & Environment 26:1419–1430.

Blaser, J., A. Sarre, D. Poore, and S. Johnson. 2011. Status of tropical forest management 2011. International Tropical Timber Organization, Yokohama, Japan.

Bohlman, S., and S. O'Brien. 2006. Allometry, adult stature and regeneration requirement of 65 tree species on Barro Colorado Island, Panama. Journal of Tropical Ecology 22: 123–136.

Boisier, J. P., P. Ciais, A. Ducharne, and M. Guimberteau. 2015. Projected strengthening of Amazonian dry season by constrained climate model simulations. Nature Climate Change 5:656–660.

Bonal, D., et al. 2008. Impact of severe dry season on net ecosystem exchange in the Neotropical rainforest of French Guiana. Global Change Biology 14:1917–1933.

Bongers, F., P. Charles-Dominique, P.-M. Forget, and M. Thery. 2001. Nouragues: dynamics and plant-animal interactions in a neotropical rainforest. Kluwer Academic Publishers, Dordrecht, The Netherlands.

Boyd, I. L., P. H. Freer-Smith, C. A. Gilligan, and H. C. J. Godfray. 2013. The consequence of tree pests and diseases for ecosystem services. Science 342:1235773.

Bréchet, L., S. Ponton, J. Roy, V. Freycon, M.-M. Coûteaux, D. Bonal, and D. Epron. 2009. Do tree species characteristics influence soil respiration in tropical forests? A test based on 16 tree species planted in monospecific plots. Plant and Soil 319:235–246.

Brienen, R. J. W., et al. 2015. Long-term decline of the Amazon carbon sink. Nature 519:344–348.

Brunner, A. 1998. A light model for spatially explicit forest stand models. Forest Ecology and Management 107:19–46.

Buchmann, N., J.-M. Guehl, T. S. Barigah, and J. R. Ehleringer. 1997. Interseasonal comparison of CO_2 concentrations, isotopic composition, and carbon dynamics in an Amazonian rainforest (French Guiana). Oecologia 110:120–131.

Bugmann, H. 2001. A review of forest gap models. Climatic Change 51:259–305.

Calders, K., T. Schenkels, H. Bartholomeus, J. Armston, J. Verbesselt, and M. Herold. 2015. Monitoring spring phenology with high temporal resolution terrestrial LiDAR measurements. Agricultural and Forest Meteorology 203:158–168.

Canham, C. D., A. C. Finzi, S. W. Pacala, and D. H. Burbank. 1994. Causes and consequences of resource heterogeneity in forests: interspecific variation in light transmission by canopy trees. Canadian Journal of Forest Research 24:337–349.

Cannell, M. G. R., and J. H. M. Thornley. 2000. Modelling the components of plant respiration: some guiding principles. Annals of Botany 85:45–54.

Cardinale, B. J., et al. 2009. Effects of biodiversity on the functioning of ecosystems: a summary of 164 experimental manipulations of species richness. Ecology 90:854.

Caughlin, T. T., S. Elliott, and J. W. Lichstein. 2016. When does seed limitation matter for scaling up reforestation from patches to landscapes? Ecological Applications 26:2439–2450.

Cavaleri, M. A., S. F. Oberbauer, and M. G. Ryan. 2006. Wood CO_2 efflux in a primary tropical rain forest. Global Change Biology 12:2442–2458.

Cavaleri, M. A., S. F. Oberbauer, and M. G. Ryan. 2008. Foliar and ecosystem respiration in an old-growth tropical rain forest. Plant, Cell & Environment 31:473–483.

Chave, J. 1999. Study of structural, successional and spatial patterns in tropical rain forests using TROLL, a spatially explicit forest model. Ecological Modelling 124:233–254.

Chave, J. 2001. Spatial patterns and persistence of woody plant species in ecological communities. American Naturalist 157: 51–65.

Chave, J., et al. 2005. Tree allometry and improved estimation of carbon stocks and balance in tropical forests. Oecologia 145:87–99.

Chave, J., et al. 2008*a*. Assessing evidence for a pervasive alteration in tropical tree communities. PLoS Biology 6:e45.

Chave, J., J. Olivier, F. Bongers, P. Châtelet, P.-M. Forget, P. van der Meer, N. Norden, B. Riéra, and P. Charles-Dominique. 2008*b*. Above-ground biomass and productivity in a rain forest of eastern South America. Journal of Tropical Ecology 24:355–366.

Chave, J., D. Coomes, S. Jansen, S. L. Lewis, N. G. Swenson, and A. E. Zanne. 2009. Towards a worldwide wood economics spectrum. Ecology Letters 12:351–366.

Chave, J., et al. 2010. Regional and seasonal patterns of litterfall in tropical South America. Biogeosciences 7:43–55.

Chave, J., et al. 2014. Improved allometric models to estimate the aboveground biomass of tropical trees. Global Change Biology 20:3177–3190.

Chazdon, R. L. 2003. Tropical forest recovery: legacies of human impact and natural disturbances. Perspectives in Plant Ecology, Evolution and Systematics 6:51–71.

Chazdon, R. L., B. Finegan, R. S. Capers, B. Salgado-Negret, F. Casanoves, V. Boukili, and N. Norden. 2010. Composition

and dynamics of functional groups of trees during tropical forest succession in northeastern Costa Rica. Biotropica 42:31–40.

Chen, G., Y. Yang, and D. Robinson. 2013. Allocation of gross primary production in forest ecosystems: allometric constraints and environmental responses. New Phytologist 200:1176–1186.

Chesson, P. 2000. Mechanisms of maintenance of species diversity. Annual Review of Ecology and Systematics 31:343–366.

Chesson, P. L., and R. R. Warner. 1981. Environmental variability promotes coexistence in lottery competitive systems. American Naturalist 117:923–943.

Chiang, J.-M., M. J. Spasojevic, H. C. Muller-Landau, I.-F. Sun, Y. Lin, S.-H. Su, Z.-S. Chen, C.-T. Chen, N. G. Swenson, and R. W. McEwan. 2016. Functional composition drives ecosystem function through multiple mechanisms in a broadleaved subtropical forest. Oecologia 182:829–840.

Chisholm, R. A., et al. 2013. Scale-dependent relationships between tree species richness and ecosystem function in forests. Journal of Ecology 101:1214–1224.

Clark, D. B., P. C. Olivas, S. F. Oberbauer, D. A. Clark, and M. G. Ryan. 2008. First direct landscape-scale measurement of tropical rain forest Leaf Area Index, a key driver of global primary productivity. Ecology Letters 11:163–172.

Clark, D. B., et al. 2011. The joint UK land environment simulator (JULES), model description – Part 2: carbon fluxes and vegetation. Geoscientific Model Development Discussions 4:641–688.

Clark, D. A., S. Asao, R. Fisher, S. Reed, P. B. Reich, M. G. Ryan, T. E. Wood, and X. Yang. 2017. Field data to benchmark the carbon-cycle models for tropical forests. Biogeosciences Discussions 2017:1–44.

Coley, P. D., J. P. Bryant, and I. I. I. F. Stuart Chapin. 1985. Resource availability and plant antiherbivore defense. Science 230:895–900.

Comita, L. S., and S. P. Hubbell. 2009. Local neighborhood and species' shade tolerance influence survival in a diverse seedling bank. Ecology 90:328–334.

Comita, L. S., H. C. Muller-Landau, S. Aguilar, and S. P. Hubbell. 2010. Asymmetric density dependence shapes species abundances in a tropical tree community. Science 329:330–332.

Comita, L. S., S. A. Queenborough, S. J. Murphy, J. L. Eck, K. Xu, M. Krishnadas, N. Beckman, and Y. Zhu. 2014. Testing predictions of the Janzen-Connell hypothesis: a meta-analysis of experimental evidence for distance- and density-dependent seed and seedling survival. Journal of Ecology 102:845–856.

Connell, J. H. 1971. On the role of natural enemies in preventing competitive exclusion in some marine animals and in rain forest trees. Pages 298–312 *in* P. J. den Boer and G. R. Gradwell, editors. Dynamics of populations. Centre for Agricultural Publishing and Documentation, Wageningen, The Netherlands.

Coomes, D. A., and P. J. Grubb. 2003. Colonization, tolerance, competition and seed-size variation within functional groups. Trends in Ecology & Evolution 18:283–291.

Courbaud, B., V. Lafond, G. Lagarrigues, G. Vieilledent, T. Cordonnier, F. Jabot, and F. de Coligny. 2015. Applying ecological model evaluation: Lessons learned with the forest dynamics model Samsara2. Ecological Modelling 314:1–14.

Cournac, L., M.-A. Dubois, J. Chave, and B. Riéra. 2002. Fast determination of light availability and leaf area index in tropical forests. Journal of Tropical Ecology 18:295–302.

Cowan, I. R., and G. D. Farquhar. 1977. Stomatal function in relation to leaf metabolism and environment. Pages 471–505 *in* D. H. Jennings, editor. Integration of activity in the higher plant. Cambridge University Press, Cambridge, UK.

Davidson, E., P. A. Lefebvre, P. M. Brando, D. M. Ray, S. E. Trumbore, L. A. Solorzano, J. N. Ferreira, M. M. C. da Bustamante, and D. C. Nepstad. 2011. Carbon inputs and water uptake in deep soils of an eastern Amazon forest. Forest Science 57:51–58.

de Almeida Castanho, A. D., D. Galbraith, K. Zhang, M. T. Coe, M. H. Costa, and P. Moorcroft. 2016. Changing Amazon biomass and the role of atmospheric CO_2 concentration, climate, and land use. Global Biogeochemical Cycles 30:2015GB005135.

De Weirdt, M., H. Verbeeck, F. Maignan, P. Peylin, B. Poulter, D. Bonal, P. Ciais, and K. Steppe. 2012. Seasonal leaf dynamics for tropical evergreen forests in a process-based global ecosystem model. Geoscientific Model Development 5:1091–1108.

Delbart, N., P. Ciais, J. Chave, N. Viovy, Y. Malhi, and T. Le Toan. 2010. Mortality as a key driver of the spatial distribution of aboveground biomass in Amazonian forest: results from a dynamic vegetation model. Biogeosciences 7:3027–3039.

Díaz, S., et al. 2016. The global spectrum of plant form and function. Nature 529:167–171.

Dietze, M. C., A. Sala, M. S. Carbone, C. I. Czimczik, J. A. Mantooth, A. D. Richardson, and R. Vargas. 2014. Nonstructural carbon in woody plants. Annual Review of Plant Biology 65:667–687.

Domingues, T. F., et al. 2010. Co-limitation of photosynthetic capacity by nitrogen and phosphorus in West Africa woodlands. Plant, Cell & Environment 33:959–980.

Domingues, T. F., L. A. Martinelli, and J. R. Ehleringer. 2014. Seasonal patterns of leaf-level photosynthetic gas exchange in an eastern Amazonian rain forest. Plant Ecology & Diversity 7:189–203.

Doughty, C. E., and M. L. Goulden. 2008. Seasonal patterns of tropical forest leaf area index and CO_2 exchange. Journal of Geophysical Research: Biogeosciences 113:G00B06.

Doughty, C. E., et al. 2014. Allocation trade-offs dominate the response of tropical forest growth to seasonal and interannual drought. Ecology 95:2192–2201.

Elias, M., and C. Potvin. 2003. Assessing inter- and intra-specific variation in trunk carbon concentration for 32 neotropical tree species. Canadian Journal of Forest Research 33:1039–1045.

Engelbrecht, B. M. J., and T. A. Kursar. 2003. Comparative drought-resistance of seedlings of 28 species of co-occurring tropical woody plants. Oecologia 136:383–393.

Espírito-Santo, F. D. B., et al. 2014. Size and frequency of natural forest disturbances and the Amazon forest carbon balance. Nature Communications 5:3434.

Ewers, R. M., A. Andrade, S. G. Laurance, J. L. Camargo, T. E. Lovejoy, and W. F. Laurance. 2017. Predicted trajectories of tree community change in Amazonian rainforest fragments. Ecography 40:26–35.

Falster, D. S., A. Brännström, U. Dieckmann, and M. Westoby. 2011. Influence of four major plant traits on average height, leaf-area cover, net primary productivity, and biomass density in single-species forests: a theoretical investigation. Journal of Ecology 99:148–164.

Fargeon, H., M. Aubry-Kientz, O. Brunaux, L. Descroix, R. Gaspard, S. Guitet, V. Rossi, and B. Hérault. 2016. Vulnerability of commercial tree species to water stress in logged forests of the Guiana Shield. Forests 7:105.

Farquhar, G. D., S. von Caemmerer, and J. A. Berry. 1980. A biochemical model of photosynthetic CO_2 assimilation in leaves of C3 species. Planta 149:78–90.

Farrior, C. E., R. Dybzinski, S. A. Levin, and S. W. Pacala. 2013. Competition for water and light in closed-canopy forests: a tractable model of carbon allocation with implications for carbon sinks. American Naturalist 181:314–330.

Farrior, C. E., S. A. Bohlman, S. Hubbell, and S. W. Pacala. 2016. Dominance of the suppressed: power-law size structure in tropical forests. Science 351:155–157.

Fatichi, S., S. Leuzinger, and C. Körner. 2014. Moving beyond photosynthesis: from carbon source to sink-driven vegetation modeling. New Phytologist 201:1086–1095.

Fauset, S., T. R. Baker, S. L. Lewis, T. R. Feldpausch, K. Affum-Baffoe, E. G. Foli, K. C. Hamer, and M. D. Swaine. 2012. Drought-induced shifts in the floristic and functional composition of tropical forests in Ghana. Ecology Letters 15:1120–1129.

Fayle, T. M., E. C. Turner, Y. Basset, R. M. Ewers, G. Reynolds, and V. Novotny. 2015. Whole-ecosystem experimental manipulations of tropical forests. Trends in Ecology & Evolution 30:334–346.

Feldpausch, T. R., C. C. da Prates-Clark, E. C. M. Fernandes, and S. J. Riha. 2007. Secondary forest growth deviation from chronosequence predictions in central Amazonia. Global Change Biology 13:967–979.

Feldpausch, T. R., et al. 2011. Height-diameter allometry of tropical forest trees. Biogeosciences 8:1081–1106.

Feldpausch, T. R., et al. 2016. Amazon forest response to repeated droughts. Global Biogeochemical Cycles 30:964–982.

Fernández-Martínez, M., et al. 2014. Nutrient availability as the key regulator of global forest carbon balance. Nature Climate Change 4:471–476.

Finegan, B., et al. 2015. Does functional trait diversity predict above-ground biomass and productivity of tropical forests? Testing three alternative hypotheses. Journal of Ecology 103:191–201.

Fischer, R., et al. 2016. Lessons learned from applying a forest gap model to understand ecosystem and carbon dynamics of complex tropical forests. Ecological Modelling 326:124–133.

Fisher, J. B., D. N. Huntzinger, C. R. Schwalm, and S. Sitch. 2014. Modeling the terrestrial biosphere. Annual Review of Environment and Resources 39:91–123.

Forister, M. L., et al. 2015. The global distribution of diet breadth in insect herbivores. Proceedings of the National Academy of Sciences USA 112:442–447.

Forrester, D. I. 2014. The spatial and temporal dynamics of species interactions in mixed-species forests: From pattern to process. Forest Ecology and Management 312:282–292.

Forrester, D. I., and X. Tang. 2016. Analysing the spatial and temporal dynamics of species interactions in mixed-species forests and the effects of stand density using the 3-PG model. Ecological Modelling 319:233–254.

Friedlingstein, P., G. Joel, C. B. Field, and I. Y. Fung. 1999. Toward an allocation scheme for global terrestrial carbon models. Global Change Biology 5:755–770.

Friedlingstein, P., M. Meinshausen, V. K. Arora, C. D. Jones, A. Anav, S. K. Liddicoat, and R. Knutti. 2013. Uncertainties in CMIP5 climate projections due to carbon cycle feedbacks. Journal of Climate 27:511–526.

Friend, A. D., et al. 2014. Carbon residence time dominates uncertainty in terrestrial vegetation responses to future climate and atmospheric CO_2. Proceedings of the National Academy of Sciences USA 111:3280–3285.

Fu, Y. S. H., M. Campioli, Y. Vitasse, H. J. D. Boeck, J. V. den Berge, H. AbdElgawad, H. Asard, S. Piao, G. Deckmyn, and I. A. Janssens. 2014. Variation in leaf flushing date influences autumnal senescence and next year's flushing date in two temperate tree species. Proceedings of the National Academy of Sciences USA 111:7355–7360.

Fyllas, N. M., et al. 2009. Basin-wide variations in foliar properties of Amazonian forest: phylogeny, soils and climate. Biogeosciences 6:2677–2708.

Fyllas, N. M., et al. 2014. Analysing Amazonian forest productivity using a new individual and trait-based model (TFS v. 1). Geoscientific Model Development 7:1251–1269.

Gastellu-Etchegorry, J. P., V. Demarez, V. Pinel, and F. Zagolski. 1996. Modeling radiative transfer in heterogeneous 3-D vegetation canopies. Remote Sensing of Environment 58:131–156.

Gleason, H. A. 1926. The individualistic concept of the plant association. Bulletin of the Torrey Botanical Club 53:7–26.

Goll, D. S., V. Brovkin, B. R. Parida, C. H. Reick, J. Kattge, P. B. Reich, P. M. van Bodegom, and Ü. Niinemets. 2012. Nutrient limitation reduces land carbon uptake in simulations with a model of combined carbon, nitrogen and phosphorus cycling. Biogeosciences 9:3547–3569.

Gonzalez, M. A., A. Roger, E. A. Courtois, F. Jabot, N. Norden, C. E. T. Paine, C. Baraloto, C. Thébaud, and J. Chave. 2010. Shifts in species and phylogenetic diversity between sapling and tree communities indicate negative density dependence in a lowland rain forest. Journal of Ecology 98:137–146.

Gourlet-Fleury, S., J.-M. Guehl, and O. Laroussinie. 2004. Ecology and management of a Neotropical rainforest: lessons drawn from Paracou, a long-term experimental research site in French Guiana. Elsevier, Paris, France.

Grace, J. B., et al. 2016. Integrative modelling reveals mechanisms linking productivity and plant species richness. Nature 529:390–393.

Granier, A., R. Huc, and S. T. Barigah. 1996. Transpiration of natural rain forest and its dependence on climatic factors. Agricultural and Forest Meteorology 78:19–29.

Granier, A., N. Bréda, P. Biron, and S. Villette. 1999. A lumped water balance model to evaluate duration and intensity of drought constraints in forest stands. Ecological Modelling 116:269–283.

Grime, J. P. 1997. Biodiversity and ecosystem function: the debate deepens. Science 277:1260–1261.

Grossiord, C., et al. 2014. Tree diversity does not always improve resistance of forest ecosystems to drought. Proceedings of the National Academy of Sciences USA 111:14812–14815.

Guan, K., et al. 2015. Photosynthetic seasonality of global tropical forests constrained by hydroclimate. Nature Geoscience 8:284–289.

Guillemot, J., C. Francois, G. Hmimina, E. Dufrêne, N. K. Martin-StPaul, K. Soudani, G. Marie, J.-M. Ourcival, and N. Delpierre. 2017. Environmental control of carbon allocation matters for modelling forest growth. New Phytologist 214:180–193.

Harfoot, M. B. J., T. Newbold, D. P. Tittensor, S. Emmott, J. Hutton, V. Lyutsarev, M. J. Smith, J. P. W. Scharlemann, and D. W. Purves. 2014. Emergent global patterns of ecosystem structure and function from a mechanistic general ecosystem model. PLoS Biology 12:e1001841.

Harms, K. E., S. J. Wright, O. Calderón, A. Hernández, and E. A. Herre. 2000. Pervasive density-dependent recruitment enhances seedling diversity in a tropical forest. Nature 404:493–495.

Harper, A., I. T. Baker, A. S. Denning, D. A. Randall, D. Dazlich, and M. Branson. 2013. Impact of evapotranspiration on dry season climate in the Amazon forest. Journal of Climate 27:574–591.

Hartig, F., J. Dyke, T. Hickler, S. I. Higgins, R. B. O'Hara, S. Scheiter, and A. Huth. 2012. Connecting dynamic vegetation models to data—an inverse perspective. Journal of Biogeography 39:2240–2252.

Hartig, F., C. Dislich, T. Wiegand, and A. Huth. 2014. Technical note: Approximate Bayesian parameterization of a process-based tropical forest model. Biogeosciences 11:1261–1272.

Heskel, M. A., et al. 2016. Convergence in the temperature response of leaf respiration across biomes and plant functional types. Proceedings of the National Academy of Sciences USA 113:3832–3837.

Hicke, J. A., et al. 2012. Effects of biotic disturbances on forest carbon cycling in the United States and Canada. Global Change Biology 18:7–34.

Hooper, D. U., et al. 2005. Effects of biodiversity on ecosystem functioning: a consensus of current knowledge. Ecological Monographs 75:3–35.

Hubbell, S. P., F. He, R. Condit, L. Borda-de-Água, J. Kellner, and H. ter Steege. 2008. How many tree species are there in the Amazon and how many of them will go extinct? Proceedings of the National Academy of Sciences USA 105:11498–11504.

Huntingford, C., et al. 2013. Simulated resilience of tropical rainforests to CO_2-induced climate change. Nature Geoscience 6:268–273.

Iida, Y., T. S. Kohyama, T. Kubo, A. R. Kassim, L. Poorter, F. Sterck, and M. D. Potts. 2011. Tree architecture and life-history strategies across 200 co-occurring tropical tree species. Functional Ecology 25:1260–1268.

Iida, Y., L. Poorter, F. J. Sterck, A. R. Kassim, T. Kubo, M. D. Potts, and T. S. Kohyama. 2012. Wood density explains architectural differentiation across 145 co-occurring tropical tree species. Functional Ecology 26:274–282.

Janzen, D. H. 1970. Herbivores and the number of tree species in tropical forests. American Naturalist 104:501–528.

Johnson, M. O., et al. 2016. Variation in stem mortality rates determines patterns of above-ground biomass in Amazonian forests: implications for dynamic global vegetation models. Global Change Biology 22:3996–4013.

Jost, L. 2006. Entropy and diversity. Oikos 113:363–375.

Jucker, T., et al. 2017. Allometric equations for integrating remote sensing imagery into forest monitoring programmes. Global Change Biology 23:177–190.

Jung, M., et al. 2011. Global patterns of land-atmosphere fluxes of carbon dioxide, latent heat, and sensible heat derived from eddy covariance, satellite, and meteorological observations. Journal of Geophysical Research: Biogeosciences 116:G00J07.

Kala, J., M. G. De Kauwe, A. J. Pitman, R. Lorenz, B. E. Medlyn, Y.-P. Wang, Y.-S. Lin, and G. Abramowitz. 2015. Implementation of an optimal stomatal conductance scheme in the Australian community climate earth systems simulator (ACCESS1.3b). Geoscientific Model Development 8:3877–3889.

Kala, J., M. G. De Kauwe, A. J. Pitman, B. E. Medlyn, Y.-P. Wang, R. Lorenz, and S. E. Perkins-Kirkpatrick. 2016. Impact of the representation of stomatal conductance on model projections of heatwave intensity. Scientific Reports 6:23418.

Kattge, J., and W. Knorr. 2007. Temperature acclimation in a biochemical model of photosynthesis: a reanalysis of data from 36 species. Plant, Cell & Environment 30:1176–1190.

Kattge, J., et al. 2011. TRY—a global database of plant traits. Global Change Biology 17:2905–2935.

King, D. A., S. J. Davies, S. Tan, and N. S. M. Noor. 2006. The role of wood density and stem support costs in the growth and mortality of tropical trees. Journal of Ecology 94:670–680.

Kitajima, K., S. S. Mulkey, and S. J. Wright. 1997. Seasonal leaf phenotypes in the canopy of a tropical dry forest: photosynthetic characteristics and associated traits. Oecologia 109:490–498.

Kitajima, K., S. S. Mulkey, M. Samaniego, and S. J. Wright. 2002. Decline of photosynthetic capacity with leaf age and position in two tropical pioneer tree species. American Journal of Botany 89:1925–1932.

Kitajima, K., S. S. Mulkey, and S. J. Wright. 2005. Variation in crown light utilization characteristics among tropical canopy trees. Annals of Botany 95:535–547.

Klein, T. 2014. The variability of stomatal sensitivity to leaf water potential across tree species indicates a continuum between isohydric and anisohydric behaviours. Functional Ecology 28:1313–1320.

Klein, T., R. T. W. Siegwolf, and C. Körner. 2016. Belowground carbon trade among tall trees in a temperate forest. Science 352:342–344.

Knauer, J., C. Werner, and S. Zaehle. 2015. Evaluating stomatal models and their atmospheric drought response in a land surface scheme: A multibiome analysis. Journal of Geophysical Research: Biogeosciences 120:2015JG003114.

Köhler, P., and A. Huth. 1998. The effects of tree species grouping in tropical rainforest modelling: simulations with the individual-based model Formind. Ecological Modelling 109:301–321.

Köhler, P., J. Chave, B. Riéra, and A. Huth. 2003. Simulating the long-term response of tropical wet forests to fragmentation. Ecosystems 6:0114–0128.

Körner, C. 2015. Paradigm shift in plant growth control. Current Opinion in Plant Biology 25:107–114.

Kraft, N. J. B., M. R. Metz, R. S. Condit, and J. Chave. 2010. The relationship between wood density and mortality in a global tropical forest data set. New Phytologist 188:1124–1136.

Lagarrigues, G., F. Jabot, V. Lafond, and B. Courbaud. 2015. Approximate Bayesian computation to recalibrate individual-based models with population data: illustration with a forest simulation model. Ecological Modelling 306:278–286.

Laio, F., A. Porporato, L. Ridolfi, and I. Rodriguez-Iturbe. 2001. Plants in water-controlled ecosystems: active role in hydrologic processes and response to water stress: II. Probabilistic soil moisture dynamics. Advances in Water Resources 24:707–723.

Laliberté, E., and P. Legendre. 2010. A distance-based framework for measuring functional diversity from multiple traits. Ecology 91:299–305.

Larpin, D. 1989. Evolution floristique et structurale d'un recrû forestier en Guyane Française. Revue d'Ecologie 44:209–224.

Lasky, J. R., M. Uriarte, V. K. Boukili, and R. L. Chazdon. 2014. Trait-mediated assembly processes predict successional changes in community diversity of tropical forests. Proceedings of the National Academy of Sciences USA 111:5616–5621.

Laughlin, D. C. 2014. The intrinsic dimensionality of plant traits and its relevance to community assembly. Journal of Ecology 102:186–193.

Laughlin, D. C., C. Joshi, P. M. van Bodegom, Z. A. Bastow, and P. Z. Fulé. 2012. A predictive model of community assembly that incorporates intraspecific trait variation. Ecology Letters 15:1291–1299.

Laurance, W. F. 2008. Theory meets reality: How habitat fragmentation research has transcended island biogeographic theory. Biological Conservation 141:1731–1744.

Laurance, W. F., L. V. Ferreira, J. M. Rankin-De Merona, and S. G. Laurance. 1998. Rain forest fragmentation and the dynamics of Amazonian tree communities. Ecology 79:2032–2040.

Laurance, W. F., J. Sayer, and K. G. Cassman. 2014. Agricultural expansion and its impacts on tropical nature. Trends in Ecology & Evolution 29:107–116.

Le Bec, J., B. Courbaud, G. L. Moguédec, and R. Pélissier. 2015. Characterizing tropical tree species growth strategies:

learning from inter-individual variability and scale invariance. PLoS One 10:e0117028.

Le Roux, X., A. Lacointe, A. Escobar-Gutiérrez, and S. L. Dizès. 2001. Carbon-based models of individual tree growth: a critical appraisal. Annals of Forest Science 58:38.

Lebrija-Trejos, E., E. A. Perez-Garcia, J. A. Meave, L. Poorter, and F. Bongers. 2011. Environmental changes during secondary succession in a tropical dry forest in Mexico. Journal of Tropical Ecology 27:477–489.

Letcher, S. G., and R. L. Chazdon. 2009. Rapid recovery of biomass, species richness, and species composition in a forest chronosequence in northeastern Costa Rica. Biotropica 41:608–617.

Letcher, S. G., R. L. Chazdon, A. C. S. Andrade, F. Bongers, M. van Breugel, B. Finegan, S. G. Laurance, R. C. G. Mesquita, M. Martínez-Ramos, and G. B. Williamson. 2012. Phylogenetic community structure during succession: evidence from three Neotropical forest sites. Perspectives in Plant Ecology, Evolution and Systematics 14:79–87.

Leuning, R. 1995. A critical appraisal of a combined stomatal-photosynthesis model for C3 plants. Plant, Cell & Environment 18:339–355.

Lewis, P. 1999. Three-dimensional plant modelling for remote sensing simulation studies using the botanical plant modelling system. Agronomie 19:185–210.

Lewis, S. L., D. P. Edwards, and D. Galbraith. 2015. Increasing human dominance of tropical forests. Science 349:827–832.

Li, L., M. L. McCormack, C. Ma, D. Kong, Q. Zhang, X. Chen, H. Zeng, Ü. Niinemets, and D. Guo. 2015. Leaf economics and hydraulic traits are decoupled in five species-rich tropical-subtropical forests. Ecology Letters 18:899–906.

Liang, J., et al. 2016. Positive biodiversity-productivity relationship predominant in global forests. Science 354:aaf8957.

Lin, Y.-S., et al. 2015. Optimal stomatal behaviour around the world. Nature Climate Change 5:459–464.

Lines, E. R., M. A. Zavala, D. W. Purves, and D. A. Coomes. 2012. Predictable changes in aboveground allometry of trees along gradients of temperature, aridity and competition. Global Ecology and Biogeography 21:1017–1028.

Lischke, H., and T. J. Löffler. 2006. Intra-specific density dependence is required to maintain species diversity in spatio-temporal forest simulations with reproduction. Ecological Modelling 198:341–361.

Lischke, H., N. E. Zimmermann, J. Bolliger, S. Rickebusch, and T. J. Löffler. 2006. TreeMig: a forest-landscape model for simulating spatio-temporal patterns from stand to landscape scale. Ecological Modelling 199:409–420.

Litton, C. M., J. W. Raich, and M. G. Ryan. 2007. Carbon allocation in forest ecosystems. Global Change Biology 13:2089–2109.

Lohbeck, M., L. Poorter, E. Lebrija-Trejos, M. Martínez-Ramos, J. A. Meave, H. Paz, E. A. Pérez-García, I. E. Romero-Pérez, A. Tauro, and F. Bongers. 2013. Successional changes in functional composition contrast for dry and wet tropical forest. Ecology 94:1211–1216.

Lohbeck, M., L. Poorter, M. Martínez-Ramos, J. Rodriguez-Velázquez, M. van Breugel, and F. Bongers. 2014. Changing drivers of species dominance during tropical forest succession. Functional Ecology 28:1052–1058.

Lohbeck, M., L. Poorter, M. Martínez-Ramos, and F. Bongers. 2015. Biomass is the main driver of changes in ecosystem process rates during tropical forest succession. Ecology 96:1242–1252.

Lohbeck, M., F. Bongers, M. Martinez-Ramos, and L. Poorter. 2016. The importance of biodiversity and dominance for multiple ecosystem functions in a human-modified tropical landscape. Ecology 97:2772–2779.

Long, S. P., W. F. Postl, and H. R. Bolhár-Nordenkampf. 1993. Quantum yields for uptake of carbon dioxide in C_3 vascular plants of contrasting habitats and taxonomic groupings. Planta 189:226–234.

Loreau, M. 1998. Separating sampling and other effects in biodiversity experiments. Oikos 82:600–602.

Loreau, M. 2010. Linking biodiversity and ecosystems: towards a unifying ecological theory. Philosophical Transactions of the Royal Society B 365:49–60.

Loreau, M., and C. de Mazancourt. 2013. Biodiversity and ecosystem stability: a synthesis of underlying mechanisms. Ecology Letters 16:106–115.

Loreau, M., and A. Hector. 2001. Partitioning selection and complementarity in biodiversity experiments. Nature 412:72–76.

Malhi, Y. 2012. The productivity, metabolism and carbon cycle of tropical forest vegetation. Journal of Ecology 100:65–75.

Malhi, Y., J. T. Roberts, R. A. Betts, T. J. Killeen, W. Li, and C. A. Nobre. 2008. Climate change, deforestation, and the fate of the Amazon. Science 319:169–172.

Malhi, Y., C. Doughty, and D. Galbraith. 2011. The allocation of ecosystem net primary productivity in tropical forests. Philosophical Transactions of the Royal Society B 366:3225–3245.

Malhi, Y., et al. 2015. The linkages between photosynthesis, productivity, growth and biomass in lowland Amazonian forests. Global Change Biology 21:2283–2295.

Maréchaux, I., M. K. Bartlett, L. Sack, C. Baraloto, J. Engel, E. Joetzjer, and J. Chave. 2015. Drought tolerance as predicted by leaf water potential at turgor loss point varies strongly across species within an Amazonian forest. Functional Ecology 29:1268–1277.

Marthews, T. R., D. F. R. P. Burslem, S. R. Paton, F. Yanyuez, and C. E. Mullins. 2008. Soil drying in a tropical forest: three distinct environments controlled by gap size. Ecological Modelling 216:369–384.

Martínez-Vilalta, J., R. Poyatos, D. Aguadé, J. Retana, and M. Mencuccini. 2014. A new look at water transport regulation in plants. New Phytologist 204:105–115.

Martínez-Vilalta, J., A. Sala, D. Asensio, L. Galiano, G. Hoch, S. Palacio, F. I. Piper, and F. Lloret. 2016. Dynamics of non-structural carbohydrates in terrestrial plants: a global synthesis. Ecological Monographs 86:495–516.

Medlyn, B. E., A. P. Robinson, R. Clement, and R. E. McMurtrie. 2005. On the validation of models of forest CO_2 exchange using eddy covariance data: some perils and pitfalls. Tree Physiology 25:839–857.

Medlyn, B. E., R. A. Duursma, D. Eamus, D. S. Ellsworth, I. C. Prentice, C. V. M. Barton, K. Y. Crous, P. De Angelis, M. Freeman, and L. Wingate. 2011. Reconciling the optimal and empirical approaches to modelling stomatal conductance. Global Change Biology 17:2134–2144.

Medlyn, B. E., et al. 2015. Using ecosystem experiments to improve vegetation models. Nature Climate Change 5:528–534.

Medlyn, B. E., et al. 2016. Using models to guide field experiments: a priori predictions for the CO_2 response of a nutrient- and water-limited native Eucalypt woodland. Global Change Biology 22:2834–2851.

Meir, P., and J. Grace. 2002. Scaling relationships for woody tissue respiration in two tropical rain forests. Plant, Cell & Environment 25:963–973.

Meir, P., J. Grace, and A. C. Miranda. 2000. Photographic method to measure the vertical distribution of leaf area density in forests. Agricultural and Forest Meteorology 102:105–111.

Meir, P., J. Grace, and A. C. Miranda. 2001. Leaf respiration in two tropical rainforests: constraints on physiology by

phosphorus, nitrogen and temperature. Functional Ecology 15:378–387.

Meir, P., T. E. Wood, D. R. Galbraith, P. M. Brando, A. C. L. D. Costa, L. Rowland, and L. V. Ferreira. 2015. Threshold responses to soil moisture deficit by trees and soil in tropical rain forests: insights from field experiments. BioScience 65:882–892.

Mencuccini, M., J. Martínez-Vilalta, D. Vanderklein, H. A. Hamid, E. Korakaki, S. Lee, and B. Michiels. 2005. Size-mediated ageing reduces vigour in trees. Ecology Letters 8:1183–1190.

Mensah, S., R. Veldtman, A. E. Assogbadjo, R. Glèlè Kakaï, and T. Seifert. 2016. Tree species diversity promotes aboveground carbon storage through functional diversity and functional dominance. Ecology and Evolution 6:7546–7557.

Mercado, L. M., N. Bellouin, S. Sitch, O. Boucher, C. Huntingford, M. Wild, and P. M. Cox. 2009*a*. Impact of changes in diffuse radiation on the global land carbon sink. Nature 458:1014–1017.

Mercado, L. M., J. Lloyd, A. J. Dolman, S. Sitch, and S. Patiño. 2009*b*. Modelling basin-wide variations in Amazon forest productivity – Part 1: model calibration, evaluation and upscaling functions for canopy photosynthesis. Biogeosciences 6:1247–1272.

Mercado, L. M., et al. 2011. Variations in Amazon forest productivity correlated with foliar nutrients and modelled rates of photosynthetic carbon supply. Philosophical Transactions of the Royal Society B 366:3316–3329.

Metcalfe, D. B., et al. 2014. Herbivory makes major contributions to ecosystem carbon and nutrient cycling in tropical forests. Ecology Letters 17:324–332.

Mokany, K., et al. 2016. Integrating modelling of biodiversity composition and ecosystem function. Oikos 125:10–19.

Moles, A. T., and M. Westoby. 2006. Seed size and plant strategy across the whole life cycle. Oikos 113:91–105.

Moles, A. T., D. S. Falster, M. R. Leishman, and M. Westoby. 2004. Small-seeded species produce more seeds per square metre of canopy per year, but not per individual per lifetime. Journal of Ecology 92:384–396.

Monteith, J. L., and M. H. Unsworth. 2008. Principles of environmental physics. Third edition. Academic Press, Amsterdam, The Netherlands.

Moorcroft, P. R. 2006. How close are we to a predictive science of the biosphere? Trends in Ecology & Evolution 21:400–407.

Moorcroft, P. R., G. C. Hurtt, and S. W. Pacala. 2001. A method for scaling vegetation dynamics: the ecosystem demography model (ED). Ecological Monographs 71:557–586.

Morin, X., L. Fahse, M. Scherer-Lorenzen, and H. Bugmann. 2011. Tree species richness promotes productivity in temperate forests through strong complementarity between species. Ecology Letters 14:1211–1219.

Morin, X., L. Fahse, C. de Mazancourt, M. Scherer-Lorenzen, and H. Bugmann. 2014. Temporal stability in forest productivity increases with tree diversity due to asynchrony in species dynamics. Ecology Letters 17:1526–1535.

Muller, B., F. Pantin, M. Génard, O. Turc, S. Freixes, M. Piques, and Y. Gibon. 2011. Water deficits uncouple growth from photosynthesis, increase C content, and modify the relationships between C and growth in sink organs. Journal of Experimental Botany 62:1715–1729.

Norby, R. J., et al. 2016. Model–data synthesis for the next generation of forest free-air CO_2 enrichment (FACE) experiments. New Phytologist 209:17–28.

Norden, N., J. Chave, P. Belbenoit, A. Caubère, P. Châtelet, P.-M. Forget, and C. Thébaud. 2007. Mast fruiting is a frequent strategy in woody species of eastern South America. PLoS ONE 2:e1079.

Norden, N., R. L. Chazdon, A. Chao, Y.-H. Jiang, and B. Vílchez-Alvarado. 2009. Resilience of tropical rain forests: tree community reassembly in secondary forests. Ecology Letters 12:385–394.

Norden, N., et al. 2015. Successional dynamics in Neotropical forests are as uncertain as they are predictable. Proceedings of the National Academy of Sciences USA 112:8013–8018.

Pacala, S. W., C. D. Canham, J. Saponara, J. A. Silander, R. K. Kobe, and E. Ribbens. 1996. Forest models defined by field measurements: estimation, error analysis and dynamics. Ecological Monographs 66:1–43.

Paine, C. E. T., N. Norden, J. Chave, P.-M. Forget, C. Fortunel, K. G. Dexter, and C. Baraloto. 2012. Phylogenetic density dependence and environmental filtering predict seedling mortality in a tropical forest. Ecology Letters 15:34–41.

Paquette, A., and C. Messier. 2011. The effect of biodiversity on tree productivity: from temperate to boreal forests. Global Ecology and Biogeography 20:170–180.

Patiño, S., N. M. Fyllas, T. R. Baker, R. Paiva, C. A. Quesada, A. J. B. Santos, M. Schwarz, H. ter Steege, O. L. Phillips, and J. Lloyd. 2012. Coordination of physiological and structural traits in Amazon forest trees. Biogeosciences 9:775–801.

Pavlick, R., D. T. Drewry, K. Bohn, B. Reu, and A. Kleidon. 2013. The Jena diversity-dynamic global vegetation model (JeDi-DGVM): a diverse approach to representing terrestrial biogeography and biogeochemistry based on plant functional trade-offs. Biogeosciences 10:4137–4177.

Peñuelas, J., et al. 2013. Human-induced nitrogen–phosphorus imbalances alter natural and managed ecosystems across the globe. Nature Communications 4:2934.

Pianosi, F., K. Beven, J. Freer, J. W. Hall, J. Rougier, D. B. Stephenson, and T. Wagener. 2016. Sensitivity analysis of environmental models: a systematic review with practical workflow. Environmental Modelling & Software 79:214–232.

Poorter, L., S. F. Oberbauer, and D. B. Clark. 1995. Leaf optical properties along a vertical gradient in a tropical rain forest canopy in Costa Rica. American Journal of Botany 82:1257–1263.

Poorter, L., M. van de Plassche, S. Willems, and R. G. A. Boot. 2004. Leaf traits and herbivory rates of tropical tree species differing in successional status. Plant Biology 6:746–754.

Poorter, L., F. Bongers, F. J. Sterck, and H. Wöll. 2005. Beyond the regeneration phase: differentiation of height–light trajectories among tropical tree species. Journal of Ecology 93:256–267.

Poorter, L., L. Bongers, and F. Bongers. 2006. Architecture of 54 moist-forest tree species: traits, trade-offs, and functional groups. Ecology 87:1289–1301.

Poorter, L., et al. 2008. Are functional traits good predictors of demographic rates? Evidence from five Neotropical forests. Ecology 89:1908–1920.

Poorter, H., Ü. Niinemets, L. Poorter, I. J. Wright, and R. Villar. 2009. Causes and consequences of variation in leaf mass per area (LMA): a meta-analysis. New Phytologist 182:565–588.

Poorter, L., et al. 2015. Diversity enhances carbon storage in tropical forests. Global Ecology and Biogeography 24:1314–1328.

Poorter, L., et al. 2016. Biomass resilience of Neotropical secondary forests. Nature 530:211–214.

Potvin, C., and N. J. Gotelli. 2008. Biodiversity enhances individual performance but does not affect survivorship in tropical trees. Ecology Letters 11:217–223.

Powers, J. S., K. K. Becklund, M. G. Gei, S. B. Iyengar, R. Meyer, C. S. O'Connell, E. M. Schilling, C. M. Smith, B. G. Waring, and L. K. Werden. 2015. Nutrient addition effects on tropical dry forests: a mini-review from microbial to ecosystem scales. Biogeoscience 3:34.

Prado-Junior, J. A., I. Schiavini, V. S. Vale, C. S. Arantes, M. T. van der Sande, M. Lohbeck, and L. Poorter. 2016.

Conservative species drive biomass productivity in tropical dry forests. Journal of Ecology 104:817–827.

Prentice, I. C., A. Bondeau, W. Cramer, S. P. Harrison, T. Hickler, W. Lucht, S. Sitch, B. Smith, and M. T. Sykes. 2007. Dynamic global vegetation modeling: Quantifying terrestrial ecosystem responses to large-scale environmental change. Pages 175–192 *in* J. G. Canadell, D. E. Pataki, and L. F. Pitelka, editors. Terrestrial ecosystems in a changing world. Springer, Berlin, Germany.

Prentice, I. C., N. Dong, S. M. Gleason, V. Maire, and I. J. Wright. 2014. Balancing the costs of carbon gain and water transport: testing a new theoretical framework for plant functional ecology. Ecology Letters 17:82–91.

Pretzsch, H., D. I. Forrester, and T. Rötzer. 2015. Representation of species mixing in forest growth models. A review and perspective. Ecological Modelling 313:276–292.

Price, D. T., et al. 2001. Regeneration in gap models: priority issues for studying forest responses to climate change. Climatic Change 51:475–508.

Purves, D., and S. Pacala. 2008. Predictive models of forest dynamics. Science 320:1452–1453.

Quesada, C. A., et al. 2010. Variations in chemical and physical properties of Amazon forest soils in relation to their genesis. Biogeosciences 7:1515–1541.

Quesada, C. A., et al. 2012. Basin-wide variations in Amazon forest structure and function are mediated by both soils and climate. Biogeosciences 9:2203–2246.

R Core Team. 2013. R: a language and environment for statistical computing. R Foundation for Statistical Computing, Vienna, Austria. www.r-project.org

Reich, P. B., M. B. Walters, and D. S. Ellsworth. 1992. Leaf lifespan in relation to leaf, plant, and stand characteristics among diverse ecosystems. Ecological Monographs 62:365–392.

Reich, P. B., M. B. Walters, and D. S. Ellsworth. 1997. From tropics to tundra: global convergence in plant functioning. Proceedings of the National Academy of Sciences USA 94:13730–13734.

Réjou-Méchain, M., B. Tymen, L. Blanc, S. Fauset, T. R. Feldpausch, A. Monteagudo, O. L. Phillips, H. Richard, and J. Chave. 2015. Using repeated small-footprint LiDAR acquisitions to infer spatial and temporal variations of a high-biomass Neotropical forest. Remote Sensing of Environment 169:93–101.

Restrepo-Coupe, N., et al. 2013. What drives the seasonality of photosynthesis across the Amazon basin? A cross-site analysis of eddy flux tower measurements from the Brasil flux network. Agricultural and Forest Meteorology 182–183:128–144.

Rogers, A., et al. 2017. A roadmap for improving the representation of photosynthesis in Earth system models. New Phytologist 213:22–42.

Rosenzweig, M. L. 1995. Species diversity in space and time. Cambridge University Press, Cambridge, UK.

Rowland, L., T. C. Hill, C. Stahl, L. Siebicke, B. Burban, J. Zaragoza-Castells, S. Ponton, D. Bonal, P. Meir, and M. Williams. 2014. Evidence for strong seasonality in the carbon storage and carbon use efficiency of an Amazonian forest. Global Change Biology 20:979–991.

Roy, J., S. Hättenschwiler, and A.-M. Domenach. 2005. Tree diversity and soil biology: a new research program in French Guyana. Pages 337–348 *in* D. Binkley and O. Menyailo, editors. Tree species effects on soils: implications for global change. Springer, Dordrecht, the Netherlands.

Rozendaal, D. M. A., and R. L. Chazdon. 2015. Demographic drivers of tree biomass change during secondary succession in northeastern Costa Rica. Ecological Applications 25:506–516.

Ruiz-Jaen, M. C., and C. Potvin. 2011. Can we predict carbon stocks in tropical ecosystems from tree diversity? Comparing species and functional diversity in a plantation and a natural forest. New Phytologist 189:978–987.

Rutishauser, E., F. Wagner, B. Herault, E.-A. Nicolini, and L. Blanc. 2010. Contrasting above-ground biomass balance in a Neotropical rain forest. Journal of Vegetation Science 21:672–682.

Ryan, M. G., R. M. Hubbard, D. A. Clark, and R. L. S. Jr. 1994. Woody-tissue respiration for *Simarouba amara* and *Minquartia guianensis*, two tropical wet forest trees with different growth habits. Oecologia 100:213–220.

Ryan, M. G., D. Binkley, and J. H. Fownes. 1997. Age-related decline in forest productivity. Advances in Ecological Research 27:213–262.

Saatchi, S. S., et al. 2011. Benchmark map of forest carbon stocks in tropical regions across three continents. Proceedings of the National Academy of Sciences USA 108:9899–9904.

Sakschewski, B., W. von Bloh, A. Boit, A. Rammig, J. Kattge, L. Poorter, J. Peñuelas, and K. Thonicke. 2015. Leaf and stem economics spectra drive diversity of functional plant traits in a dynamic global vegetation model. Global Change Biology 21:2711–2725.

Sala, A., D. R. Woodruff, and F. C. Meinzer. 2012. Carbon dynamics in trees: feast or famine? Tree Physiology 32:764–775.

Saldarriaga, J. G., D. C. West, M. L. Tharp, and C. Uhl. 1988. Long-term chronosequence of forest succession in the upper Rio Negro of Colombia and Venezuela. Journal of Ecology 76:938–958.

Sapijanskas, J., A. Paquette, C. Potvin, N. Kunert, and M. Loreau. 2014. Tropical tree diversity enhances light capture through crown plasticity and spatial and temporal niche differences. Ecology 95:2479–2492.

Sato, H., A. Itoh, and T. Kohyama. 2007. SEIB-DGVM: a new dynamic global vegetation model using a spatially explicit individual-based approach. Ecological Modelling 200:279–307.

Scheffers, B. R., L. N. Joppa, S. L. Pimm, and W. F. Laurance. 2012. What we know and don't know about Earth's missing biodiversity. Trends in Ecology & Evolution 27:501–510.

Scheiter, S., and S. I. Higgins. 2009. Impacts of climate change on the vegetation of Africa: an adaptive dynamic vegetation modelling approach. Global Change Biology 15:2224–2246.

Scheiter, S., L. Langan, and S. I. Higgins. 2013. Next-generation dynamic global vegetation models: learning from community ecology. New Phytologist 198:957–969.

Scherer-Lorenzen, M., E.-D. Schulze, A. Don, J. Schumacher, and E. Weller. 2007. Exploring the functional significance of forest diversity: a new long-term experiment with temperate tree species (BIOTREE). Perspectives in Plant Ecology, Evolution and Systematics 9:53–70.

Schippers, P., M. Vlam, P. A. Zuidema, and F. Sterck. 2015. Sapwood allocation in tropical trees: a test of hypotheses. Functional Plant Biology 42:697–709.

Schmitz, O. J. 2003. Top predator control of plant biodiversity and productivity in an old-field ecosystem. Ecology Letters 6:156–163.

Sevanto, S., N. G. Mcdowell, L. T. Dickman, R. Pangle, and W. T. Pockman. 2014. How do trees die? A test of the hydraulic failure and carbon starvation hypotheses. Plant, Cell & Environment 37:153–161.

Sheil, D., D. F. R. P. Burslem, and D. Alder. 1995. The interpretation and misinterpretation of mortality rate measures. Journal of Ecology 83:331–333.

Shugart, H. H. 1984. A theory of forest dynamics. Springer, New York, New York, USA.

Shugart, H. H., G. P. Asner, R. Fischer, A. Huth, N. Knapp, T. Le Toan, and J. K. Shuman. 2015. Computer and remote-sensing infrastructure to enhance large-scale testing of individual-based forest models. Frontiers in Ecology and the Environment 13:503–511.

Sitch, S., et al. 2003. Evaluation of ecosystem dynamics, plant geography and terrestrial carbon cycling in the LPJ dynamic global vegetation model. Global Change Biology 9:161–185.

Slot, M., S. J. Wright, and K. Kitajima. 2013. Foliar respiration and its temperature sensitivity in trees and lianas: in situ measurements in the upper canopy of a tropical forest. Tree Physiology 33:505–515.

Smith, N. G., and J. S. Dukes. 2013. Plant respiration and photosynthesis in global-scale models: incorporating acclimation to temperature and CO_2. Global Change Biology 19:45–63.

Snell, R. S., et al. 2014. Using dynamic vegetation models to simulate plant range shifts. Ecography 37:1184–1197.

Stahl, C., B. Burban, F. Bompy, Z. B. Jolin, J. Sermage, and D. Bonal. 2010. Seasonal variation in atmospheric relative humidity contributes to explaining seasonal variation in trunk circumference of tropical rain-forest trees in French Guiana. Journal of Tropical Ecology 26:393–405.

Stahl, C., B. Burban, J.-Y. Goret, and D. Bonal. 2011. Seasonal variations in stem CO_2 efflux in the Neotropical rainforest of French Guiana. Annals of Forest Science 68:771–782.

Stephenson, N. L., et al. 2014. Rate of tree carbon accumulation increases continuously with tree size. Nature 507:90–93.

Sterck, F. J., L. Poorter, and F. Schieving. 2006. Leaf traits determine the growth-survival trade-off across rain forest tree species. American Naturalist 167:758–765.

Strigul, N., D. Pristinski, D. Purves, J. Dushoff, and S. Pacala. 2008. Scaling from trees to forests: tractable macroscopic equations for forest dynamics. Ecological Monographs 78:523–545.

Sullivan, M. J. P., et al. 2017. Diversity and carbon storage across the tropical forest biome. Scientific Reports 7:39102.

Terborgh, J., et al. 2001. Ecological meltdown in predator-free forest fragments. Science 294:1923–1926.

ter Steege, H., et al. 2006. Continental-scale patterns of canopy tree composition and function across Amazonia. Nature 443:444–447.

Thomas, S. C., and A. R. Martin. 2012. Carbon content of tree tissues: a synthesis. Forests 3:332–352.

Thornley, J. H. M., and M. G. R. Cannell. 2000. Modelling the components of plant respiration: representation and realism. Annals of Botany 85:55–67.

Tobner, C. M., A. Paquette, P. B. Reich, D. Gravel, and C. Messier. 2013. Advancing biodiversity–ecosystem functioning science using high-density tree-based experiments over functional diversity gradients. Oecologia 174:609–621.

Toïgo, M., P. Vallet, T. Perot, J.-D. Bontemps, C. Piedallu, and B. Courbaud. 2015. Overyielding in mixed forests decreases with site productivity. Journal of Ecology 103:502–512.

Uriarte, M., R. Condit, C. D. Canham, and S. P. Hubbell. 2004. A spatially explicit model of sapling growth in a tropical forest: does the identity of neighbours matter? Journal of Ecology 92:348–360.

Uriarte, M., C. D. Canham, J. Thompson, J. K. Zimmerman, L. Murphy, A. M. Sabat, N. Fetcher, and B. L. Haines. 2009. Natural disturbance and human land use as determinants of tropical forest dynamics: results from a forest simulator. Ecological Monographs 79:423–443.

van Bodegom, P. M., J. C. Douma, J. P. M. Witte, J. C. Ordoñez, R. P. Bartholomeus, and R. Aerts. 2012. Going beyond limitations of plant functional types when predicting global ecosystem–atmosphere fluxes: exploring the merits of traits-based approaches. Global Ecology and Biogeography 21:625–636.

van Bodegom, P. M., J. C. Douma, and L. M. Verheijen. 2014. A fully traits-based approach to modeling global vegetation distribution. Proceedings of the National Academy of Sciences 111:13733–13738.

van der Meer, P. J., and F. Bongers. 1996. Patterns of tree-fall and branch-fall in a tropical rain forest in French Guiana. Journal of Ecology 84:19–29.

van der Sande, M. T., P. A. Zuidema, and F. Sterck. 2015. Explaining biomass growth of tropical canopy trees: the importance of sapwood. Oecologia 177:1145–1155.

van der Sande, M. T., et al. 2016. Old-growth Neotropical forests are shifting in species and trait composition. Ecological Monographs 86:228–243.

Verheijen, L. M., V. Brovkin, R. Aerts, G. Bönisch, J. H. C. Cornelissen, J. Kattge, P. B. Reich, I. J. Wright, and P. M. van Bodegom. 2013. Impacts of trait variation through observed trait–climate relationships on performance of an Earth system model: a conceptual analysis. Biogeosciences 10:5497–5515.

Vilà, M., J. Vayreda, L. Comas, J. J. Ibáñez, T. Mata, and B. Obón. 2007. Species richness and wood production: a positive association in Mediterranean forests. Ecology Letters 10:241–250.

Visser, M. D., M. Bruijning, S. J. Wright, H. C. Muller-Landau, E. Jongejans, L. S. Comita, and H. de Kroon. 2016. Functional traits as predictors of vital rates across the life cycle of tropical trees. Functional Ecology 30:168–180.

von Caemmerer, S. 2000. Biochemical models of leaf photosynthesis. CSIRO Publishing, Collingwood, Australia.

Wagner, F. H., et al. 2016. Climate seasonality limits leaf carbon assimilation and wood productivity in tropical forests. Biogeosciences 13:2537.

Weerasinghe, L. K., D. Creek, K. Y. Crous, S. Xiang, M. J. Liddell, M. H. Turnbull, and O. K. Atkin. 2014. Canopy position affects the relationships between leaf respiration and associated traits in a tropical rainforest in Far North Queensland. Tree Physiology 34:564–584.

Westoby, M. 1998. A leaf-height-seed (LHS) plant ecology strategy scheme. Plant and Soil 199:213–227.

Widlowski, J.-L., et al. 2013. The fourth radiation transfer model intercomparison (RAMI-IV): proficiency testing of canopy reflectance models with ISO-13528. Journal of Geophysical Research: Atmospheres 118:6869–6890.

Williams, M., E. B. Rastetter, D. N. Fernandes, M. L. Goulden, S. C. Wofsy, G. R. Shaver, J. M. Melillo, J. W. Munger, S.-M. Fan, and K. J. Nadelhoffer. 1996. Modelling the soil-plant-atmosphere continuum in a *Quercus–Acer* stand at Harvard Forest: the regulation of stomatal conductance by light, nitrogen and soil/plant hydraulic properties. Plant, Cell & Environment 19:911–927.

Wirth, R., B. Weber, and R. J. Ryel. 2001. Spatial and temporal variability of canopy structure in a tropical moist forest. Acta Oecologica 22:235–244.

Woodruff, D. R., and F. C. Meinzer. 2011. Water stress, shoot growth and storage of non-structural carbohydrates along a tree height gradient in a tall conifer. Plant, Cell & Environment 34:1920–1930.

Wright, J. S. 2002. Plant diversity in tropical forests: a review of mechanisms of species coexistence. Oecologia 130:1–14.

Wright, I. J., et al. 2004. The worldwide leaf economics spectrum. Nature 428:821–827.

Wright, I. J., P. B. Reich, O. K. Atkin, C. H. Lusk, M. G. Tjoelker, and M. Westoby. 2006. Irradiance, temperature and

rainfall influence leaf dark respiration in woody plants: evidence from comparisons across 20 sites. New Phytologist 169:309–319.

Wright, S. J., et al. 2010. Functional traits and the growth–mortality trade-off in tropical trees. Ecology 91:3664–3674.

Wright, S. J., et al. 2011. Potassium, phosphorus, or nitrogen limit root allocation, tree growth, or litter production in a lowland tropical forest. Ecology 92:1616–1625.

Wu, J., et al. 2016. Leaf development and demography explain photosynthetic seasonality in Amazon evergreen forests. Science 351:972–976.

Yoda, K., K. Shinozaki, H. Ogawa, K. Hozumi, and T. Kira. 1965. Estimation of the total amount of respiration in woody organs of trees and forest communities. Journal of Biology of Osaka City University 16:15–26.

Zaehle, S., S. Sitch, B. Smith, and F. Hatterman. 2005. Effects of parameter uncertainties on the modeling of terrestrial biosphere dynamics. Global Biogeochemical Cycles 19:GB3020.

Zhu, Y., L. S. Comita, S. P. Hubbell, and K. Ma. 2015. Conspecific and phylogenetic density-dependent survival differs across life stages in a tropical forest. Journal of Ecology 103:957–966.

Supporting Information

Additional supporting information may be found online at: http://onlinelibrary.wiley.com/doi/10.1002/ecm.1271/full